EUROPEAN ORGANIZATION FOR NUCLEAR RESEARCH (CERN)

CERN-PH-EP/2014-039
2014/04/23

CMS-SUS-13-002

Search for anomalous production of events with three or more leptons in pp collisions at $\sqrt{s} = 8\,\text{TeV}$

The CMS Collaboration*

Abstract

A search for physics beyond the standard model in events with at least three leptons is presented. The data sample, corresponding to an integrated luminosity of $19.5\,\text{fb}^{-1}$ of proton-proton collisions with center-of-mass energy $\sqrt{s} = 8\,\text{TeV}$, was collected by the CMS experiment at the LHC during 2012. The data are divided into exclusive categories based on the number of leptons and their flavor, the presence or absence of an opposite-sign, same-flavor lepton pair (OSSF), the invariant mass of the OSSF pair, the presence or absence of a tagged bottom-quark jet, the number of identified hadronically decaying τ leptons, and the magnitude of the missing transverse energy and of the scalar sum of jet transverse momenta. The numbers of observed events are found to be consistent with the expected numbers from standard model processes, and limits are placed on new-physics scenarios that yield multilepton final states. In particular, scenarios that predict Higgs boson production in the context of supersymmetric decay chains are examined. We also place a 95% confidence level upper limit of 1.3% on the branching fraction for the decay of a top quark to a charm quark and a Higgs boson ($t \to cH$), which translates to a bound on the left- and right-handed top-charm flavor-violating Higgs Yukawa couplings, λ_{tc}^{H} and λ_{ct}^{H}, respectively, of $\sqrt{|\lambda_{tc}^{H}|^2 + |\lambda_{ct}^{H}|^2} < 0.21$.

Submitted to Physical Review D

*See Appendix A for the list of collaboration members

1 Introduction

The recent discovery of a Higgs boson [1–3] at the relatively low mass of about 125 GeV implies that physics beyond the standard model (BSM) may be observable at energy scales of around 1 TeV. Supersymmetry (SUSY) is a prominent candidate for BSM physics because it provides a solution to the hierarchy problem, predicts gauge-coupling unification, and contains a "natural" candidate for dark matter [4–6]. Supersymmetry postulates the existence of fermionic superpartners for each standard model (SM) boson, and of bosonic superpartners for each SM fermion. For example, gluinos, squarks, and winos are the superpartners of gluons, quarks, and W bosons, respectively. The superparter of a lepton is a slepton. In R-parity [7] conserving SUSY models, supersymmetric particles are created in pairs, and the lightest supersymmetric particle (LSP) is stable. If the LSP interacts only weakly, as in the case of a dark matter candidate, it escapes detection, leading to missing transverse energy ($E_{\mathrm{T}}^{\mathrm{miss}}$). Here, R-parity is defined by $R = (-1)^{3B+L+2s}$, with B and L the baryon and lepton numbers, and s the particle spin. All SM particles have $R = +1$ while all superpartners have $R = -1$.

A wide range of BSM scenarios predict multilepton final states [8], where by "multilepton", we mean three or more charged leptons. Since multilepton states are relatively rare in the SM, searches in the multilepton channel have good potential to uncover BSM physics.

Given the rich SUSY particle spectrum, multilepton final states in SUSY events take on multiple forms. For example, a cascade of particles initiated by the decay of a heavy gluino can proceed through intermediate squarks, winos, and sleptons to produce a final state that is democratic in lepton flavor, i.e., equally likely to contain electrons, muons, or τ leptons. A gluino-initiated cascade can also yield a multilepton state dominated by τ leptons should the superpartner of the τ lepton (stau) be substantially lighter than the partners of the electron and muon (selectron and smuon, respectively), as is expected in some models. Another path to a multileptonic final state arises from top-squark production in which the top squark decays to leptonically-decaying third-generation quarks and to a Z boson that yields an opposite-sign same-flavor (OSSF) lepton pair. In these latter events, bottom-quark jets (b jets) might also be present. Similarly, many other multileptonic signatures are possible.

Besides SUSY, other BSM scenarios can yield multileptonic final states, such as $\mathrm{t} \to \mathrm{cH}$ transitions, with t a top quark, c a charm quark and H a Higgs boson. The $\mathrm{t} \to \mathrm{cH}$ process is extremely rare in the SM but can be enhanced through the production of new particles in loops [9, 10]. The top quark is the heaviest SM particle, and is thus the SM particle that is most strongly coupled to the Higgs boson. Since the $\mathrm{t} \to \mathrm{cH}$ process directly probes the flavor-violating couplings of the top quark to the Higgs boson, it provides a powerful means to search for BSM physics regardless of the underlying new-physics mechanism. The $\mathrm{t} \to \mathrm{cH}$ decay can give rise to a multilepton signature when a top quark in a top quark-antiquark ($\mathrm{t\bar{t}}$) pair decays to the cH state, followed by the decay of the Higgs boson to leptons through, e.g., $\mathrm{H} \to \mathrm{ZZ}^*$ or $\mathrm{H} \to \mathrm{WW}^*$ decays, in conjunction with the leptonic decay of the other top quark in the $\mathrm{t\bar{t}}$ pair.

In this paper, we present a search for BSM physics in multilepton channels. The search is based on a sample of proton-proton collision data collected at $\sqrt{s} = 8$ TeV with the Compact Muon Solenoid (CMS) detector at the CERN Large Hadron Collider (LHC) in 2012, corresponding to an integrated luminosity of $19.5\,\mathrm{fb}^{-1}$. The study is an extension of our earlier work [11], which was based on a data set of $5.0\,\mathrm{fb}^{-1}$ collected at $\sqrt{s} = 7$ TeV. A related search, presented in Ref. [12], uses the 8 TeV data set to investigate R-parity-violating SUSY scenarios. Ref. [13] presents recent results from the ATLAS Collaboration on multilepton final states.

Because of the wide range of possible BSM signatures, we have adopted a search strategy that

is sensitive to different kinematical and topological signatures, rather than optimizing the analysis for a particular model. We retain all observed multilepton candidate events and classify them into multiple mutually exclusive categories based on the number of leptons, the lepton flavor, the presence of b jets, the presence of an OSSF pair indicative of a Z boson, and kinematic characteristics such as $E_{\mathrm{T}}^{\mathrm{miss}}$ and H_{T}, where H_{T} is the scalar sum of jet transverse momentum (p_{T}) values. We then confront a number of BSM scenarios that exhibit diverse characteristics with respect to the population of these categories.

This paper is organized as follows. In Section 2, a brief summary of the CMS detector and a description of the trigger is presented. Section 3 discusses the event reconstruction procedures, event selection, and event simulation. The search strategy and the background evaluation methods are outlined in Sections 4 and 5. Section 6 contains a discussion of systematic uncertainties. The results are presented in Section 7. Sections 8 and 9 present the interpretations of our results for SUSY scenarios and for the $\mathrm{t} \to \mathrm{cH}$ process, respectively. A summary is given in Section 10.

2 Detector and trigger

The CMS detector has cylindrical symmetry around the direction of the beam axis. The coordinate system is defined with the origin at the nominal collision point and the z axis along the direction of the counterclockwise proton beam. The x axis points toward the center of the LHC ring and the y axis vertically upwards. The polar angle θ is measured with respect to the z axis. The azimuthal angle ϕ is measured in the $x - y$ plane, relative to the x axis. Both angles are measured in radians. Pseudorapidity η is defined as $\eta = -\ln[\tan(\theta/2)]$. The central feature of the detector is a superconducting solenoidal magnet of field strength 3.8 T. Within the field volume are a silicon pixel and strip tracker, a lead tungstate crystal calorimeter, and a brass-and-scintillator hadron calorimeter. The tracking detector covers the region $|\eta| < 2.5$ and the calorimeters $|\eta| < 3.0$. Muon detectors based on gas-ionization detectors lie outside the solenoid, covering $|\eta| < 2.4$. A steel-and-quartz-fiber forward calorimeter covers $|\eta| < 5.0$. A detailed description of the detector can be found in Ref. [14].

A double-lepton trigger (ee, $\mu\mu$, or eμ) is used for data collection. At the trigger level, the leptons with the highest and second-highest transverse momentum are required to satisfy $p_{\mathrm{T}} > 17\,\mathrm{GeV}$ and $p_{\mathrm{T}} > 8\,\mathrm{GeV}$, respectively. The lepton trigger efficiency is determined using an independent data sample based on minimum requirements for H_{T} [11]. After application of all selection requirements, the trigger efficiencies are found to be 95%, 90%, and 93%, respectively, for the ee, $\mu\mu$, and eμ triggers. Corrections are applied to account for the trigger inefficiencies.

3 Event reconstruction, selection, and simulation

The particle-flow (PF) method [15, 16] is used to reconstruct the physics objects used in this analysis: electrons, muons, hadronically decaying τ leptons (τ_{h}), jets, and $E_{\mathrm{T}}^{\mathrm{miss}}$.

Electrons and muons are reconstructed using measured quantities from the tracker, calorimeter, and muon system. The candidate tracks must satisfy quality requirements and spatially match energy deposits in the electromagnetic calorimeter or tracks in the muon detectors, as appropriate. Details of the reconstruction and identification procedures can be found in Ref. [17] for electrons and in Ref. [18] for muons.

Hadronically decaying τ leptons predominantly yield either a single charged track (one-prong decays) or three charged tracks (three-prong decays) with or without additional electromag-

netic energy from neutral-pion decays. Both one-prong and three-prong τ_h decays are reconstructed using the hadron plus strips (HPS) algorithm [19].

The event primary vertex is defined to be the reconstructed vertex with the largest sum of charged-track p_T^2 value and is required to lie within 24 cm of the origin in the direction along the z axis and 2 cm in the transverse plane.

Jets are formed from reconstructed PF objects using the anti-k_T algorithm [20, 21] with a distance parameter of 0.5. Corrections are applied as a function of jet p_T and η to account for non-uniform detector response [22]. Contributions to the jet p_T values due to overlapping pp interactions from the same or neighboring bunch crossing ("pileup") are subtracted using the jet area method described in Ref. [23].

Finally, E_T^{miss} is the magnitude of the vector sum of the transverse momenta of all PF objects.

We require the presence of at least three reconstructed leptons, where by "lepton" we mean an electron, muon, or τ_h candidate. Electron and muon candidates must satisfy $p_T > 10$ GeV and $|\eta| < 2.4$. At least one electron or muon candidate must satisfy $p_T > 20$ GeV. The τ_h candidates must satisfy $p_T > 20$ GeV and $|\eta| < 2.3$. Events are allowed to contain at most one τ_h candidate. Leptonically decaying τ leptons populate the electron and muon channels.

Leptons from BSM processes are typically isolated, i.e., separated in $\Delta R \equiv \sqrt{(\Delta\eta)^2 + (\Delta\phi)^2}$ from other physics objects. To reduce background from the semileptonic decays of heavy quark flavors, which generally yield leptons within jets, we apply lepton isolation criteria. For electrons and muons, we define the relative isolation I_{rel} to be the sum of the p_T values of all PF objects within a cone of radius $\Delta R = 0.3$ around the lepton direction (excluding the lepton itself), divided by the lepton p_T value, and require $I_{rel} < 0.15$. For τ_h leptons, the sum of energy $E_{iso}^{\tau_h}$ within a cone of radius $\Delta R = 0.5$ around the lepton direction is required to satisfy $E_{iso}^{\tau_h} < 2$ GeV. In all cases, we account for the effects of pileup interactions [23].

The signal scenarios contain prompt leptons, where by "prompt" we mean that the parent particles decay near the primary vertex. To ensure that the electrons and muons are prompt, their distance of closest approach to the primary vertex is required to be less than 2 cm in the direction along the beam axis and 0.02 cm in the transverse plane.

We construct OSSF pairs from charged lepton $\ell^+\ell^-$ combinations, with ℓ an electron or muon. Events with an OSSF pair that satisfies $m_{\ell^+\ell^-} < 12$ GeV are rejected to eliminate background from low-mass Drell–Yan processes and J/ψ and Υ decays. If there is more than one OSSF pair in the event, this requirement is applied to each pair. Events with an OSSF pair outside the Z boson mass region (defined by $75 < m_{\ell^+\ell^-} < 105$ GeV) but that satisfy $75 < m_{\ell^+\ell^-\ell^{(\prime)\pm}} < 105$ GeV, where $\ell^{(\prime)\pm}$ is an electron or muon with the same (different) flavor as the OSSF pair, are likely to arise from final-state photon radiation from the Z-boson decay products, followed by conversion of the photon to a charged lepton pair. Events that meet this condition are rejected if they also exhibit kinematic characteristics consistent with background from events with a Z boson and jets (Z+jets background).

Jets are required to satisfy $p_T > 30$ GeV and $|\eta| < 2.5$ and are rejected if they lie within a distance $\Delta R = 0.3$ from a lepton that satisfies our selection criteria. The identification of b jets is performed using the CMS combined secondary-vertex algorithm [24] at the medium working point. This working point yields a tagging efficiency of roughly 70% for jets with a p_T value of 80 GeV, with a misidentification rate for light-flavor events of less than 2% and for charm-quark jets of roughly 20%.

Samples of simulated events are used to determine signal acceptance and to evaluate some SM

backgrounds. The simulation of SM events is based on the MADGRAPH (version 5.1.3.30) [25] event generator with leading-order CTEQ6L1 [26] parton distribution functions (PDF), with the GEANT4 [27] package used to describe detector response. The cross sections are normalized to next-to-leading (NLO) order [28–30]. The simulation of signal events is performed using both the MADGRAPH and PYTHIA (version 6.420) [31] generators, with the description of detector response based on the CMS fast simulation program [32]. Parton showering for all simulated events is described using PYTHIA. The simulated events are adjusted to account for the multiplicity of pileup interactions observed in the data, as well as for differences between data and simulation for the jet energy scale, rate of events with initial-state radiation (ISR) [33], and b-jet tagging efficiency [24].

4 Multilepton event classification

Multilepton event candidates are separated into mutually exclusive search channels. The level of the SM background varies considerably between the different categories. The overall sensitivity to new physics is maximized by separating the low- and high-background channels. Events with exactly three leptons generally suffer from a higher background level than events with four or more leptons, as do events with a τ_h candidate. We therefore categorize events with three leptons separately from those with four or more, and events with a τ_h candidate separately from those without such a candidate. Similarly, events with a tagged b jet suffer higher background from $t\bar{t}$ events, and so are categorized separately from events without a tagged b jet.

We also define categories based on the number n of OSSF dilepton pairs that can be formed using each lepton candidate only once (OSSFn). For example, both $\mu^+\mu^-\mu^-$ and $\mu^+\mu^-e^-$ events fall into the OSSF1 category, while $\mu^+\mu^+e^-$ and $\mu^+\mu^-e^+e^-$ events fall into the OSSF0 and OSSF2 categories, respectively. Events with an OSSF pair exhibit larger levels of background than do OSSF0 events.

We further classify events with at least one OSSF pair as being "on-Z" if the reconstructed invariant mass $m_{\ell^+\ell^-}$ of any of the OSSF dilepton pairings in the event lies in the Z-boson mass region $75 < m_{\ell^+\ell^-} < 105\,\text{GeV}$. Since there is considerably less SM background above the Z-boson region than below it, we also define "above-Z" and "below-Z" categories, but for three-lepton events only, where for above-Z (below-Z) events all possible OSSF pairs satisfy $m_{\ell^+\ell^-} > 105\,\text{GeV}$ ($m_{\ell^+\ell^-} < 75\,\text{GeV}$). Additionally, we classify events with four leptons as being "off-Z" if all possible OSSF pairs have $m_{\ell^+\ell^-}$ values outside the Z-boson mass region.

Events with SUSY production of squarks and gluinos are characterized by a high level of hadronic activity compared to SM events. We therefore separate events according to whether H_T is larger or smaller than 200 GeV. Similarly, we subdivide events into five E_T^{miss} bins: four bins of width 50 GeV from 0 to 200 GeV, and a fifth bin with $E_T^{miss} > 200\,\text{GeV}$.

5 Background estimation

5.1 Overview

The largest background category for trilepton events arises from Z+jets events in which the Z boson decays to a lepton pair while the third lepton candidate is either a misidentified hadron or a genuine lepton from heavy-flavor decay. This background dominates the low-E_T^{miss} and low-H_T channels. As described below (Sections 5.2, 5.3, and 5.6), this background is evaluated from data.

Search channels with τ_h candidates suffer from higher background compared to those with only electrons and muons because sufficiently narrow jets tend to mimic hadronically decaying τ leptons. We measure the background due to misidentified τ_h decays from data (Section 5.3).

Background events containing three or more prompt genuine leptons and a significant level of E_T^{miss} can arise from SM processes such as WZ+jets or ZZ+jets production if both electroweak bosons decay leptonically. This type of background is referred to as "irreducible" because its characteristics are similar to the search signature. We use simulation to estimate the irreducible background (Section 5.4). Comparison between data and simulation demonstrates that the E_T^{miss} distribution is well modeled for processes with genuine E_T^{miss}, viz., SM model processes with neutrinos [18, 34].

Another major source of background is $t\bar{t}$ production in which each top quark produces a W boson that decays leptonically, with a third lepton arising from the semileptonic decay of the b-jet daughter of one of the two top quarks. The character of this background differs significantly from the background due to Z+jets events, in which the jets are relatively soft. Simulation is used to evaluate the $t\bar{t}$ background (Section 5.5).

Two varieties of photon conversion are relevant to consider. "External" conversion of an on-shell photon in the detector material predominantly results in an e^+e^- pair, which is eliminated using a collection of tracking and kinematic criteria appropriate to the small opening angle of the pair. In contrast, the "internal" or "Dalitz" conversion of a virtual photon produces a $\mu^+\mu^-$ pair almost as often as an e^+e^- pair. When an internal conversion is also asymmetric, i.e., when one of the leptons has a very low p_T value, the low p_T track can fail to be reconstructed or to satisfy the selection criteria. Drell–Yan processes accompanied by the high-p_T lepton from an asymmetric conversion constitute a significant source of background for trilepton channels. We estimate this background from data (Section 5.6).

Remaining backgrounds arise from rare SM processes such as triple-boson production or $t\bar{t}$ production in association with a vector boson and are estimated from simulation.

In the following subsections we describe the estimation of main SM backgrounds.

5.2 Misidentified prompt and isolated electrons and muons

Processes such as $Z(\to 2\ell)$ + jets and $W^+W^-(\to 2\ell)$ + jets predominantly generate dilepton final states. However, rare fluctuations in the hadronization process of an accompanying jet can provide a third prompt and isolated lepton, contributing to the background in the trilepton event category. Simulation of rare fragmentation processes can be unreliable. Therefore, we use dilepton data to evaluate this background [11, 35].

Consider a dilepton data sample, such as an e^+e^- sample, that shares attributes such as the E_T^{miss} and H_T values with a trilepton search channel such as $e^+e^-\mu$. The number of background events in the $e^+e^-\mu$ channel that originate from e^+e^- dilepton events is given by the number of misidentified isolated muons in the e^+e^- sample. We estimate this number to be the product of the observed number of isolated tracks in the dilepton sample and a proportionality factor f_μ between isolated tracks and muons. The factor f_μ depends on the selection requirements of the search channel and, in particular, its heavy-flavor content. Since the impact parameters of tracks are generally larger for heavy-flavor decays than for light-flavor (pion and kaon) decays, the average impact parameter value of non-isolated tracks is a good indicator of the heavy-quark content. Therefore, we characterize the variation of f_μ from sample to sample as a function of the average impact parameter value of non-isolated tracks in the dilepton sample.

The factor f_μ is determined in a procedure [11] that considers the numbers of non-isolated muons and tracks in the dilepton samples. We use the difference between cross checks performed with ee and $\mu\mu$ samples to evaluate a systematic uncertainty. From a sample of $Z(\to e^+e^-)$ + jets events, we determine $f_\mu = (0.6 \pm 0.2)\%$, where the uncertainty is systematic. Using an analogous procedure with a sample of $Z(\to \mu^+\mu^-)$ + jets events, we find $f_e = (0.7 \pm 0.2)\%$ for the background from misidentified electron candidates.

5.3 Misidentified τ_h leptons

The probability to misidentify an isolated τ_h lepton is determined by calculating an extrapolation ratio f_τ defined by the number of τ_h candidates in the isolation-variable signal region $E_{iso}^{\tau_h} < 2.0\,GeV$ to the number in a sideband region $6.0 < E_{iso}^{\tau_h} < 15.0\,GeV$ for an event sample in which no genuine τ_h leptons are expected, namely Z+jets events with $Z \to e^+e^-$ or $\mu^+\mu^-$. The extrapolation ratio is sensitive to the level of jet activity in an event. We study the variation of this ratio with respect to H_T and the number of jets, using a variety of jet-triggered and dilepton samples, and assign a systematic uncertainty of 30% based on the observed variation. Using this procedure we obtain $f_\tau = (20 \pm 6)\%$.

To estimate the τ_h background in a search channel, the number of candidates in the isolation sideband region of the corresponding dilepton sample is multiplied by the extrapolation ratio, analogously to the procedure for f_μ described in Section 5.2 for the background from misidentified electrons and muons.

5.4 Irreducible background from WZ and ZZ production

The irreducible background, from WZ+jets and ZZ+jets events where both electroweak bosons decay leptonically, is evaluated using samples of simulated events corrected for the measured lepton reconstruction efficiency and E_T^{miss} resolution. The simulated WZ and ZZ distributions are normalized to corresponding measured results obtained from WZ- and ZZ-dominated data control samples, defined by selecting events with on-Z, low-H_T, and $50 < E_T^{miss} < 100\,GeV$ requirements, or two-on-Z, low-H_T, and $E_T^{miss} < 50\,GeV$ requirements, respectively. The normalization factors have statistical uncertainties of 6% and 12%, again respectively.

The E_T^{miss} distribution is examined in individual two-dimensional bins of H_T and the number of reconstructed vertices in the event. In an individual bin, the x and y components of E_T^{miss} are found to be approximately Gaussian. The E_T^{miss} resolution is adversely affected by both pileup and jet activity, but in different ways. The effects of pileup are stochastic, affecting the Gaussian widths of the distributions, while jet activity affects the tails. We apply smearing factors to the Gaussian widths of the simulated events so that the E_T^{miss} resolution matches that of the data. The corrections to the widths vary from a few percent to as high as around 25% depending on the bin. The effects of jet activity are accounted for in the evaluation of systematic uncertainties, which are determined by varying the smearing factors and assessing the level of migration between different bins of E_T^{miss} and H_T.

For purposes of validation, Fig. 1 shows the distribution of E_T^{miss} for an on-Z, low-H_T, trilepton (eee, eeμ, e$\mu\mu$, and $\mu\mu\mu$), WZ-dominated data control sample defined by $75 < m_{\ell^+\ell^-} < 105\,GeV$, $H_T < 200\,GeV$, and $50 < M_T < 100\,GeV$, where M_T is the transverse mass [36] formed from the E_T^{miss} vector and the lepton not belonging to the OSSF pair. The results are shown in comparison to simulated results that include the above-mentioned corrections.

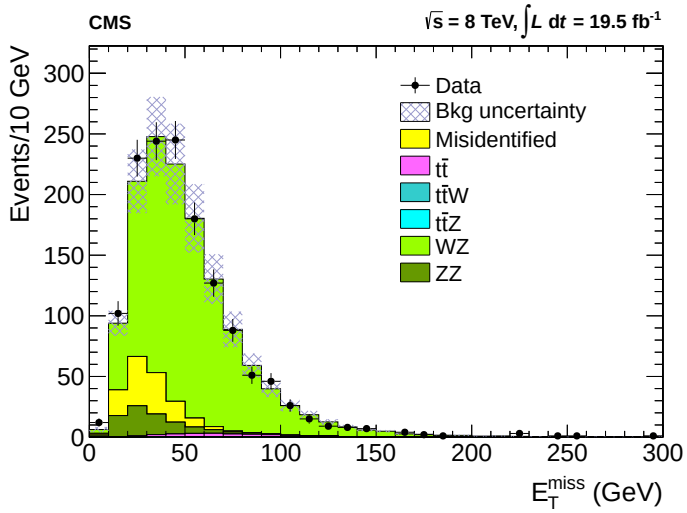

Figure 1: Distribution of $E_{\mathrm{T}}^{\mathrm{miss}}$ for a WZ-enriched data control sample, in comparison to the result from simulation. "Misidentified" refers to SM background from Drell–Yan events, misidentified τ_{h} decays, and internal photon conversions. The simulation is normalized to a control region in data.

5.5 Background from $t\bar{t}$ production

The background from $t\bar{t}$ events is evaluated from simulation, with corrections applied for lepton efficiencies and $E_{\mathrm{T}}^{\mathrm{miss}}$ resolution as described in Section 5.4. Figure 2 shows the distributions of $E_{\mathrm{T}}^{\mathrm{miss}}$ and H_{T} for the data and corrected simulation in a $t\bar{t}$-enriched control sample selected by requiring events to contain an opposite-sign eμ pair and a tagged b jet.

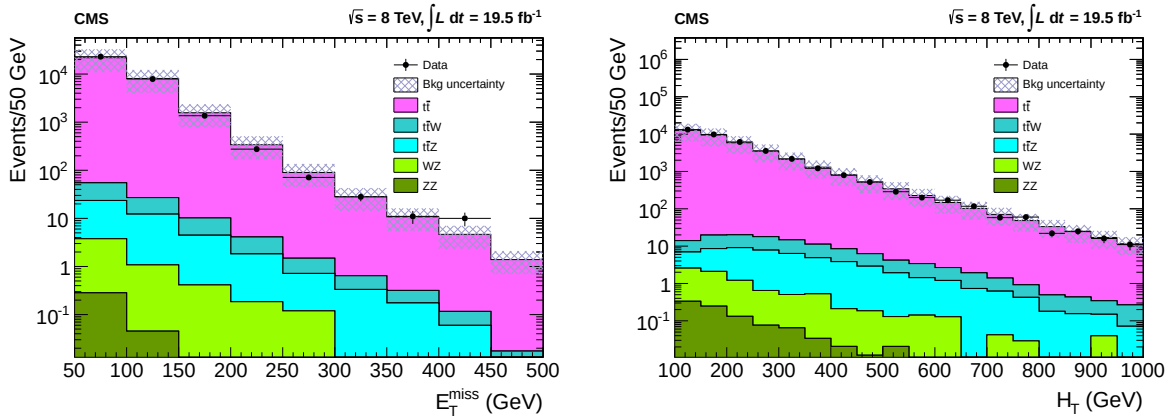

Figure 2: Distribution of (left) $E_{\mathrm{T}}^{\mathrm{miss}}$ and (right) H_{T} for a $t\bar{t}$-enriched data control sample, in comparison to the result from simulation.

5.6 Backgrounds from asymmetric internal photon conversions

The background from photon conversions is evaluated from data by selecting a low-$E_{\mathrm{T}}^{\mathrm{miss}}$, low-$H_{\mathrm{T}}$ control region defined by $E_{\mathrm{T}}^{\mathrm{miss}} < 30\,\mathrm{GeV}$ and $H_{\mathrm{T}} < 200\,\mathrm{GeV}$ and measuring the ratio of the number of events with $|m_{\ell^+\ell^-\ell'^{\pm}} - m_{\mathrm{Z}}| < 15\,\mathrm{GeV}$ to those with $|m_{\ell^+\ell^-\gamma} - m_{\mathrm{Z}}| < 15\,\mathrm{GeV}$. We find a result of $(2.0 \pm 0.3)\%$ for electrons and $(0.7 \pm 0.1)\%$ for muons, where the uncertainty is statistical. We multiply these factors by the measured $\ell^+\ell^-\gamma$ rates in the signal regions to estimate the rate of photon-conversion background events in these regions, with a systematic uncertainty of 50%.

6 Systematic uncertainties

The evaluation of systematic uncertainties for the SM background is partially discussed in the previous section. In this section, we discuss additional sources of uncertainty, both for the background estimates and the signal predictions.

Simulated signal and background samples are subject to uncertainties from the trigger, lepton-identification, and isolation requirements. The latter two uncertainties are combined into a single term that is approximately 1.5% for leptons with $p_T > 20\,\text{GeV}$. The trigger efficiency uncertainties are approximately 5%. Uncertainties associated with the jet energy scale [22], b-jet tagging efficiency [24], E_T^{miss} resolution, and luminosity [37] affect signal efficiencies as well as background estimates determined from simulation. The signal efficiencies are subject to an additional uncertainty, from the ISR modeling [33]. Uncertainties in the cross section calculations affect the signal samples and simulation-derived background estimates, with the exception of the background from WZ and ZZ production, whose normalization is determined from data.

We assign a 50% uncertainty to the estimate of the misidentified lepton background arising from $t\bar{t}$ production, which is a combination of the uncertainty attributed to the cross section and an uncertainty derived from the level of agreement between data and simulation for the distribution of the isolation variable.

The total systematic uncertainty per channel varies between 3% and 40%. Table 1 list representative values for some of the individual terms.

Table 1: Typical values for systematic uncertainties.

Source of uncertainty	Magnitude (%)
Luminosity	2.6
ISR modeling	0–5
E_T^{miss} resolution for WZ events	~ 4
Jet energy scale (WZ)	0.5
b-jet tagging	0.1 (WZ), 6 ($t\bar{t}$)
Muon ID/isolation at 10 (100) GeV	11 (0.2)
Electron ID/isolation at 10 (100) GeV	14 (0.6)
τ_h-lepton ID/isolation at 10 (100) GeV	2 (1.1)
Trigger efficiency	5
$t\bar{t}$ cross section/isolation variable	50

7 Results

Table 2 presents the results of the searches for events with four or more leptons, and Table 3 the results for exactly three leptons. The observed numbers of events are seen to be in overall agreement with the SM expectations.

Three excesses in the data relative to the SM estimates are worth noting in Table 2. All concern events in the OSSF1, off-Z category with one τ_h-lepton candidate, no tagged b jet, and $H_T < 200\,\text{GeV}$. Specifically, we observe 15, 4, and 3 events for $0 < E_T^{miss} < 50\,\text{GeV}$, $50 < E_T^{miss} < 100\,\text{GeV}$, and $E_T^{miss} > 100\,\text{GeV}$, respectively, when only 7.5 ± 2.0, 2.1 ± 0.5, and 0.60 ± 0.24 SM events are expected, for an expectation of 10.1 ± 2.4 events in the combined E_T^{miss} range. We determine the single-measurement probability to observe 22 or more events when the expected number is 10.1 ± 2.4 events to be about 1%. However, once trial factors are incorporated to

account for the 64 independent channels of the analysis, the probability to observe such a fluctuation increases to about 50%. Alternatively, the joint probability to observe at least as large an excess for all three channels considered individually is about 5%. We account for systematic uncertainties and their correlations when evaluating these probabilities.

Table 2: Observed numbers of events with four or more leptons in comparison with the estimated numbers of SM background events. "On-Z" refers to events with at least one e^+e^- or $\mu^+\mu^-$ (OSSF) pair with dilepton mass between 75 and 105 GeV, while "Off-Z" refers to events with one or two OSSF pairs, none of which fall in this mass range. The OSSF*n* designation refers to the number of e^+e^- and $\mu^+\mu^-$ pairs in the event, as explained in the text. Search channels binned in E_T^{miss} have been combined into coarse E_T^{miss} bins for the purposes of presentation. All uncertainties include both the statistical and systematic terms. The channel marked with an asterisk is used for normalization purposes and is excluded from the search.

$\geq$4 leptons	$m_{\ell^+\ell^-}$	E_T^{miss}	$N_{\tau_h}=0$, $N_b=0$		$N_{\tau_h}=1$, $N_b=0$		$c_{\tau_h}=0$, $N_b\geq 1$		$N_{\tau_h}=1$, $N_b\geq 1$	
$H_T > 200$ GeV		(GeV)	Obs.	Exp.	Obs.	Exp.	Obs.	Exp.	Obs.	Exp.
OSSF0	—	(100, ∞)	0	$0.01^{+0.03}_{-0.01}$	0	$0.01^{+0.06}_{-0.01}$	0	$0.02^{+0.04}_{-0.02}$	0	0.11 ± 0.08
OSSF0	—	(50, 100)	0	$0.00^{+0.02}_{-0.00}$	0	$0.01^{+0.06}_{-0.01}$	0	$0.00^{+0.03}_{-0.00}$	0	0.12 ± 0.07
OSSF0	—	(0, 50)	0	$0.00^{+0.02}_{-0.00}$	0	$0.07^{+0.10}_{-0.07}$	0	$0.00^{+0.02}_{-0.00}$	0	0.02 ± 0.02
OSSF1	Off-Z	(100, ∞)	0	$0.01^{+0.02}_{-0.01}$	1	0.25 ± 0.11	0	0.13 ± 0.08	0	0.12 ± 0.12
OSSF1	On-Z	(100, ∞)	1	0.10 ± 0.06	0	0.50 ± 0.27	0	0.42 ± 0.22	0	0.42 ± 0.19
OSSF1	Off-Z	(50, 100)	0	0.07 ± 0.06	1	0.29 ± 0.13	0	0.04 ± 0.04	0	0.23 ± 0.13
OSSF1	On-Z	(50, 100)	0	0.23 ± 0.11	1	0.70 ± 0.31	0	0.23 ± 0.13	1	0.34 ± 0.16
OSSF1	Off-Z	(0, 50)	0	$0.02^{+0.03}_{-0.02}$	0	0.27 ± 0.12	0	$0.03^{+0.04}_{-0.03}$	0	0.31 ± 0.15
OSSF1	On-Z	(0, 50)	0	0.20 ± 0.08	0	1.3 ± 0.5	0	0.06 ± 0.04	1	0.49 ± 0.19
OSSF2	Off-Z	(100, ∞)	0	$0.01^{+0.02}_{-0.01}$	—	—	0	$0.01^{+0.06}_{-0.01}$	—	—
OSSF2	On-Z	(100, ∞)	1	$0.15^{+0.16}_{-0.15}$	—	—	0	0.34 ± 0.18	—	—
OSSF2	Off-Z	(50, 100)	0	0.03 ± 0.02	—	—	0	0.13 ± 0.09	—	—
OSSF2	On-Z	(50, 100)	0	0.80 ± 0.40	—	—	0	0.36 ± 0.19	—	—
OSSF2	Off-Z	(0, 50)	1	0.27 ± 0.13	—	—	0	0.08 ± 0.05	—	—
OSSF2	On-Z	(0, 50)	5	7.4 ± 3.5	—	—	2	0.80 ± 0.40	—	—
$\geq$4 leptons	$m_{\ell^+\ell^-}$	E_T^{miss}	$N_{\tau_h}=0$, $N_b=0$		$N_{\tau_h}=1$, $N_b=0$		$N_{\tau_h}=0$, $N_b\geq 1$		$N_{\tau_h}=1$, $N_b\geq 1$	
$H_T < 200$ GeV		(GeV)	Obs.	Exp.	Obs.	Exp.	Obs.	Exp.	Obs.	Exp.
OSSF0	—	(100, ∞)	0	0.11 ± 0.08	0	0.17 ± 0.10	0	$0.03^{+0.04}_{-0.03}$	0	0.04 ± 0.04
OSSF0	—	(50, 100)	0	$0.01^{+0.03}_{-0.01}$	2	0.70 ± 0.33	0	$0.00^{+0.02}_{-0.00}$	0	0.28 ± 0.16
OSSF0	—	(0, 50)	0	$0.01^{+0.02}_{-0.01}$	1	0.7 ± 0.3	0	$0.00^{+0.02}_{-0.00}$	0	0.13 ± 0.08
OSSF1	Off-Z	(100, ∞)	0	0.06 ± 0.04	3	0.60 ± 0.24	0	$0.02^{+0.04}_{-0.02}$	0	0.32 ± 0.20
OSSF1	On-Z	(100, ∞)	1	0.50 ± 0.18	2	2.5 ± 0.5	1	0.38 ± 0.20	0	0.21 ± 0.10
OSSF1	Off-Z	(50, 100)	0	0.18 ± 0.06	4	2.1 ± 0.5	0	0.16 ± 0.08	1	0.45 ± 0.24
OSSF1	On-Z	(50, 100)	2	1.2 ± 0.3	9	9.6 ± 1.6	2	0.42 ± 0.23	0	0.50 ± 0.16
OSSF1	Off-Z	(0, 50)	2	0.46 ± 0.18	15	7.5 ± 2.0	0	0.09 ± 0.06	0	0.70 ± 0.31
OSSF1	On-Z	(0, 50)	4	3.0 ± 0.8	41	40 ± 10	1	0.31 ± 0.15	2	1.50 ± 0.47
OSSF2	Off-Z	(100, ∞)	0	0.04 ± 0.03	—	—	0	0.05 ± 0.04	—	—
OSSF2	On-Z	(100, ∞)	0	0.34 ± 0.15	—	—	0	0.46 ± 0.25	—	—
OSSF2	Off-Z	(50, 100)	2	0.18 ± 0.13	—	—	0	$0.02^{+0.03}_{-0.02}$	—	—
OSSF2	On-Z	(50, 100)	4	3.9 ± 2.5	—	—	0	0.50 ± 0.21	—	—
OSSF2	Off-Z	(0, 50)	7	8.9 ± 2.4	—	—	1	0.23 ± 0.09	—	—
OSSF2	On-Z	(0, 50)	*156	160 ± 34	—	—	4	2.9 ± 0.8	—	—

8 Interpretation of results for supersymmetric scenarios

We consider five new-physics scenarios that appear in the framework of the minimal supersymmetric standard model (MSSM) [4, 5]. They involve sleptons (including staus), bottom and top squarks, higgsinos, gravitinos, neutralinos, and charginos, where higgsinos are the superpartners of the Higgs bosons, the gravitino $\widetilde{G}$ is the superpartner of the graviton, while neutralinos (charginos) are mixtures of the superpartners of neutral (charged) electroweak vector

Table 3: Observed numbers of events with exactly three leptons in comparison with the estimated numbers of SM background events. "On-Z" refers to events with an e^+e^- or $\mu^+\mu^-$ (OSSF) pair with dilepton mass between 75 and 105 GeV, while "Above-Z" and "Below-Z" refer to events with an OSSF pair with mass above 105 GeV or below 75 GeV, respectively. The OSSFn designation refers to the number of e^+e^- and $\mu^+\mu^-$ pairs in the event, as explained in the text. Search channels binned in E_T^{miss} have been combined into coarse E_T^{miss} bins for the purposes of presentation. All uncertainties include both the statistical and systematic terms. The channels marked with an asterisk are used for normalization purposes and are excluded from the search.

3 leptons	$m_{\ell^+\ell^-}$	E_T^{miss}	$N_{\tau_h}=0$, $N_b=0$		$N_{\tau_h}=1$, $N_b=0$		$N_{\tau_h}=0$, $N_b\geq 1$		$N_{\tau_h}=1$, $N_b\geq 1$	
$H_T > 200$ GeV		(GeV)	Obs.	Exp.	Obs.	Exp.	Obs.	Exp.	Obs.	Exp.
OSSF0	—	(100, ∞)	5	3.7 ± 1.6	35	33 ± 14	1	5.5 ± 2.2	47	61 ± 30
OSSF0	—	(50, 100)	3	3.5 ± 1.4	34	36 ± 16	8	7.7 ± 2.7	82	91 ± 46
OSSF0	—	(0, 50)	4	2.1 ± 0.8	25	25 ± 10	1	3.6 ± 1.5	52	59 ± 29
OSSF1	Above-Z	(100, ∞)	5	3.6 ± 1.2	2	10.0 ± 4.8	3	4.7 ± 1.6	19	22 ± 11
OSSF1	Below-Z	(100, ∞)	7	9.7 ± 3.3	18	14.0 ± 6.4	8	9.1 ± 3.4	21	23 ± 11
OSSF1	On-Z	(100, ∞)	39	61 ± 23	17	15.0 ± 4.9	9	14.0 ± 4.4	10	12.0 ± 5.8
OSSF1	Above-Z	(50, 100)	4	5.0 ± 1.6	14	11.0 ± 5.2	6	6.8 ± 2.4	32	30 ± 15
OSSF1	Below-Z	(50, 100)	10	11.0 ± 3.8	24	19.0 ± 6.4	10	9.9 ± 3.7	25	32 ± 16
OSSF1	On-Z	(50, 100)	78	80 ± 32	70	50 ± 11	22	22.0 ± 6.3	36	24.0 ± 9.8
OSSF1	Above-Z	(0, 50)	3	7.3 ± 2.0	41	33.0 ± 8.7	4	5.3 ± 1.5	15	23 ± 11
OSSF1	Below-Z	(0, 50)	26	25.0 ± 6.8	110	86 ± 23	5	10.0 ± 2.5	24	26 ± 11
OSSF1	On-Z	(0, 50)	*135	130 ± 41	542	540 ± 160	31	32.0 ± 6.5	86	75 ± 19
3 leptons	$m_{\ell^+\ell^-}$	E_T^{miss}	$N_{\tau_h}=0$, $N_b=0$		$N_{\tau_h}=1$, $N_b=0$		$N_{\tau_h}=0$, $N_b\geq 1$		$N_{\tau_h}=1$, $N_b\geq 1$	
$H_T < 200$ GeV		(GeV)	Obs.	Exp.	Obs.	Exp.	Obs.	Exp.	Obs.	Exp.
OSSF0	—	(100, ∞)	7	11.0 ± 4.9	101	111 ± 54	13	10.0 ± 5.3	87	119 ± 61
OSSF0	—	(50, 100)	35	38 ± 15	406	402 ± 152	29	26 ± 13	269	298 ± 151
OSSF0	—	(0, 50)	53	51 ± 11	910	1035 ± 255	29	23 ± 10	237	240 ± 113
OSSF1	Above-Z	(100, ∞)	18	13.0 ± 3.5	25	38 ± 18	10	6.5 ± 2.9	24	35 ± 18
OSSF1	Below-Z	(100, ∞)	21	24 ± 9	41	50 ± 25	14	20 ± 10	42	54 ± 28
OSSF1	On-Z	(100, ∞)	150	150 ± 26	39	48 ± 13	15	14.0 ± 4.8	19	23 ± 11
OSSF1	Above-Z	(50, 100)	50	46.0 ± 9.7	169	140 ± 48	20	18 ± 8	85	93 ± 47
OSSF1	Below-Z	(50, 100)	142	130 ± 27	353	360 ± 92	48	48 ± 23	140	133 ± 68
OSSF1	On-Z	(50, 100)	*773	780 ± 120	1276	1200 ± 310	56	47 ± 13	81	75 ± 32
OSSF1	Above-Z	(0, 50)	178	200 ± 35	1676	1900 ± 540	17	18.0 ± 6.7	115	94 ± 42
OSSF1	Below-Z	(0, 50)	510	560 ± 87	9939	9000 ± 2700	34	42 ± 11	226	228 ± 63
OSSF1	On-Z	(0, 50)	*3869	4100 ± 670	*50188	50000 ± 15000	*148	156 ± 24	906	925 ± 263

and Higgs bosons. The first three scenarios feature the gravitino as the LSP, while the lightest neutralino $\widetilde{\chi}_1^0$ is the LSP for the other two scenarios. The first and last two scenarios proceed through the production of third-generation squarks, yielding final states rich in heavy-flavor jets. Taken together, these five scenarios present a wide spectrum of multilepton signatures.

Our search results lack striking departures from the SM, and we set limits on the production cross sections of the five scenarios. The limits are determined using the observed numbers of events, the SM background estimates, and the predicted event yields. For each scenario, we order the search channels by their expected sensitivities and then combine channels, starting with the most sensitive one. For ease of computation and with a negligible loss in overall sensitivity, we do not consider channels once the number of signal events integrated over the retained channels reaches 90% of the total. The list of selected channels thus depends not only on the scenario considered, but also on the assumed superpartner masses and branching fractions.

We set 95% confidence level (CL) upper limits on the signal parameters and cross sections using the modified frequentest CL_s method with the LHC-style test statistic [38–40]. Lognormal nuisance-parameter distributions are used to account for uncertainties.

8.1 Natural higgsino NLSP scenario

We first present a supersymmetric scenario in which the $\widetilde{\chi}_1^0$ neutralino is a higgsino that forms the next-to-LSP (NLSP) state [41]. We refer to this scenario as the "natural higgsino NLSP" scenario. This scenario arises in gauge-mediated SUSY-breaking (GMSB) models [42]. Production proceeds through the right-handed top-antitop squark pair $\bar{\widetilde{t}}_R\widetilde{t}_R^*$, with the subsequent decays $\bar{\widetilde{t}}_R \to b\widetilde{\chi}_1^+$ or $\bar{\widetilde{t}}_R \to t\widetilde{\chi}_i^0$ $(i = 1, 2)$, where $\widetilde{\chi}_1^+$ is the lightest chargino and $\widetilde{\chi}_2^0$ the second-lightest neutralino (both taken to be higgsinos), with the $\tilde{q}^*$ state the charge conjugate of the $\tilde{q}$ state. The $\widetilde{\chi}_1^+$ and $\widetilde{\chi}_2^0$ states each decay to the $\widetilde{\chi}_1^0$ and SM particles. Figure 3 shows an event diagram and a schematic mass spectrum. The last step in each of the two top-squark decay chains is the decay $\widetilde{\chi}_1^0 \to H\widetilde{G}$ or $Z\widetilde{G}$, yielding an HH, HZ, or ZZ configuration, with E_T^{miss} from the undetected gravitino. Note that we assume $H\widetilde{G}$ and $Z\widetilde{G}$ to be the only two possible decay modes for the $\widetilde{\chi}_1^0$ higgsino [42].

Beyond the top-squark pair production diagram of Fig. 3, the natural higgsino NLSP scenario also encompasses direct higgsino pair production, in which the $\widetilde{\chi}_1^+$ and $\widetilde{\chi}_1^-$ states of Fig. 3 (plus other di-higgsino states) are produced through electroweak interactions, leading to the same HH, HZ, and ZZ configuration as in Fig. 3, but with less jet activity [42]. Our search results are also sensitive to this scenario.

Of the five new-physics scenarios we examine, the natural higgsino NLSP scenario exhibits the largest range with respect to its population of the different search channels. The channels with highest sensitivity are those that require b jets, and, for the decays through the HZ and ZZ states, the channels with on-Z and off-Z requirements.

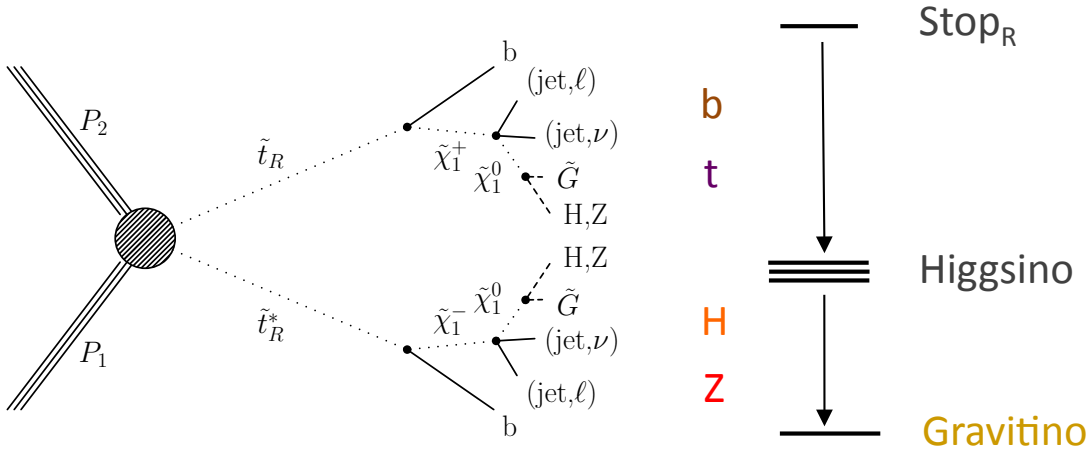

Figure 3: Event diagram and a schematic superpartner mass spectrum for the GMSB natural higgsino NLSP scenario, with $\widetilde{\chi}_1^\pm$ ($\widetilde{\chi}_1^0$) the lightest chargino (neutralino), H the lightest MSSM Higgs boson, and $\widetilde{G}$ a gravitino. Particles in parenthesis in the event diagram have a soft p_T spectrum.

The natural higgsino NLSP scenario is complex because the higgsino can decay to either a Z or Higgs boson, while the Higgs boson has many decay modes that lead to leptons. We consider seven decay channels for the HH configuration: WW^*WW^*, ZZ^*ZZ^*, $\tau\tau\tau\tau$, WW^*ZZ^*, $WW^*\tau\tau$, $ZZ^*\tau\tau$, and ZZ^*bb, and three decay channels for the HZ configuration: WW^*Z, ZZ^*Z, and $\tau\tau Z$, where W^* and Z^* indicate off-shell vector bosons.

Signal events for the natural higgsino NLSP scenario are generated using MADGRAPH, as described in Section 3. The $\widetilde{\chi}_1^0$ and $\widetilde{\chi}_2^0$ higgsinos are assigned masses 5 GeV below and above the

mass of the $\widetilde{\chi}_1^{\pm}$ higgsino, respectively, while the gravitino is assumed to be massless. We generate signal events for a range of $\bar{\widetilde{t}}_R$ and $\widetilde{\chi}_1^{\pm}$ mass values. Cross sections for both the strong and electroweak production processes are assigned an uncertainty of 20%, which also accounts for the uncertainties associated with the PDFs and with the renormalization and factorization scales.

Figure 4 shows the excluded regions in the plane of $m_{\widetilde{\chi}_1^{\pm}}$ versus $m_{\bar{\widetilde{t}}}$. The results are shown for several choices for the $\widetilde{\chi}_1^0 \to \mathrm{H}\widetilde{\mathrm{G}}$ branching fraction. One-dimensional exclusion plots with fixed choices for the branching fraction and chargino mass are shown in Fig. 5. The search sensitivity is larger for lower chargino masses because of the larger cross section. There is less sensitivity for the Higgs-boson-dominated mode in comparison with the Z-boson-dominated mode. Figure 6 shows the results as a function of the $\widetilde{\chi}_1^0 \to \mathrm{H}\widetilde{\mathrm{G}}$ branching fraction and the top squark mass for different chargino masses.

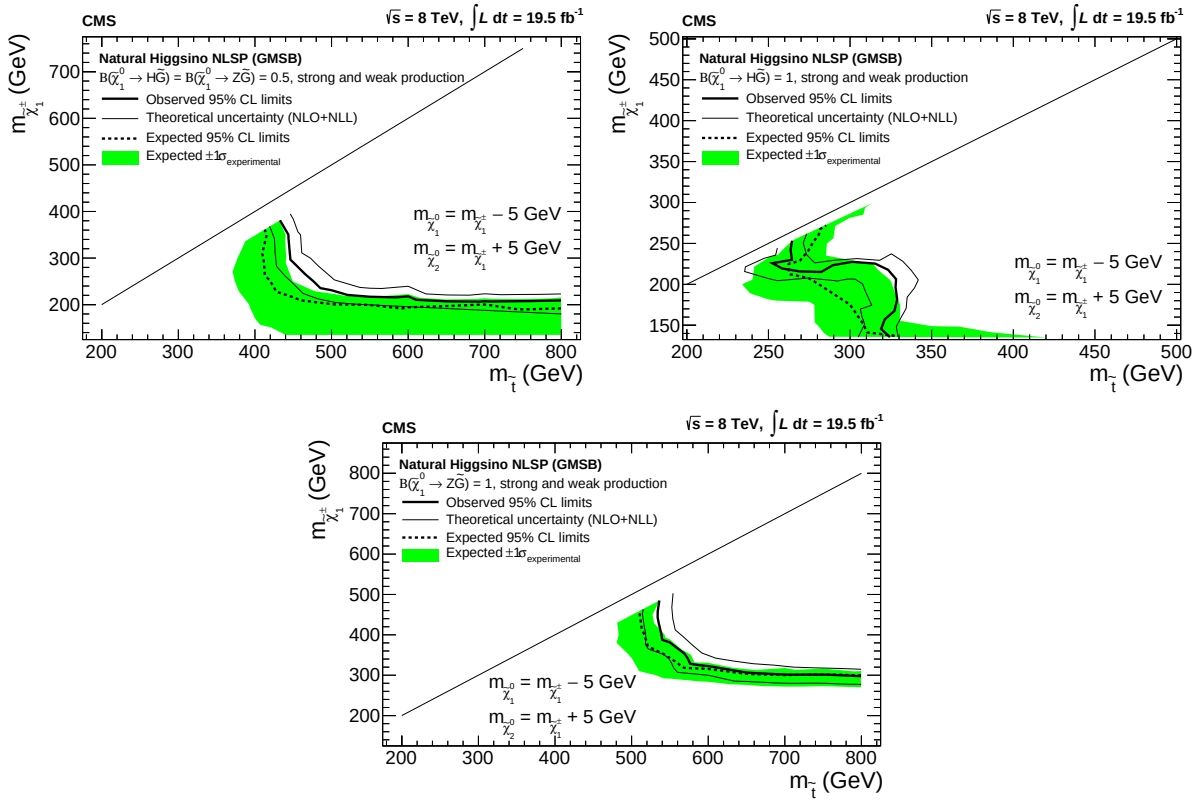

Figure 4: The 95% confidence level upper limits in the top squark versus chargino mass plane, for the natural higgsino NLSP scenario with the following $\widetilde{\chi}_1^0$ branching fractions: $\mathcal{B}(\widetilde{\chi}_1^0 \to \mathrm{H}\widetilde{\mathrm{G}}) = \mathcal{B}(\widetilde{\chi}_1^0 \to \mathrm{Z}\widetilde{\mathrm{G}}) = 0.5$ (upper left), $\mathcal{B}(\widetilde{\chi}_1^0 \to \mathrm{H}\widetilde{\mathrm{G}}) = 1.0$ (upper right), and $\mathcal{B}(\widetilde{\chi}_1^0 \to \mathrm{Z}\widetilde{\mathrm{G}}) = 1.0$ (bottom). Both strong and electroweak production mechanisms are considered. The region to the left and below the contours is excluded. The region above the diagonal straight line is unphysical.

8.2 Slepton co-NLSP scenario

We next consider the slepton co-NLSP scenario [40, 41], in which mass-degenerate right-handed sleptons $\widetilde{\ell}_R$ (selectron, smuon, stau) serve together as the NLSP. This scenario arises in a broad class of GMSB models and can lead to a multilepton final state [43–46]. The process proceeds primarily through gluino $\widetilde{\mathrm{g}}$ and squark $\widetilde{\mathrm{q}}$ pair production [47]. An event diagram and schematic

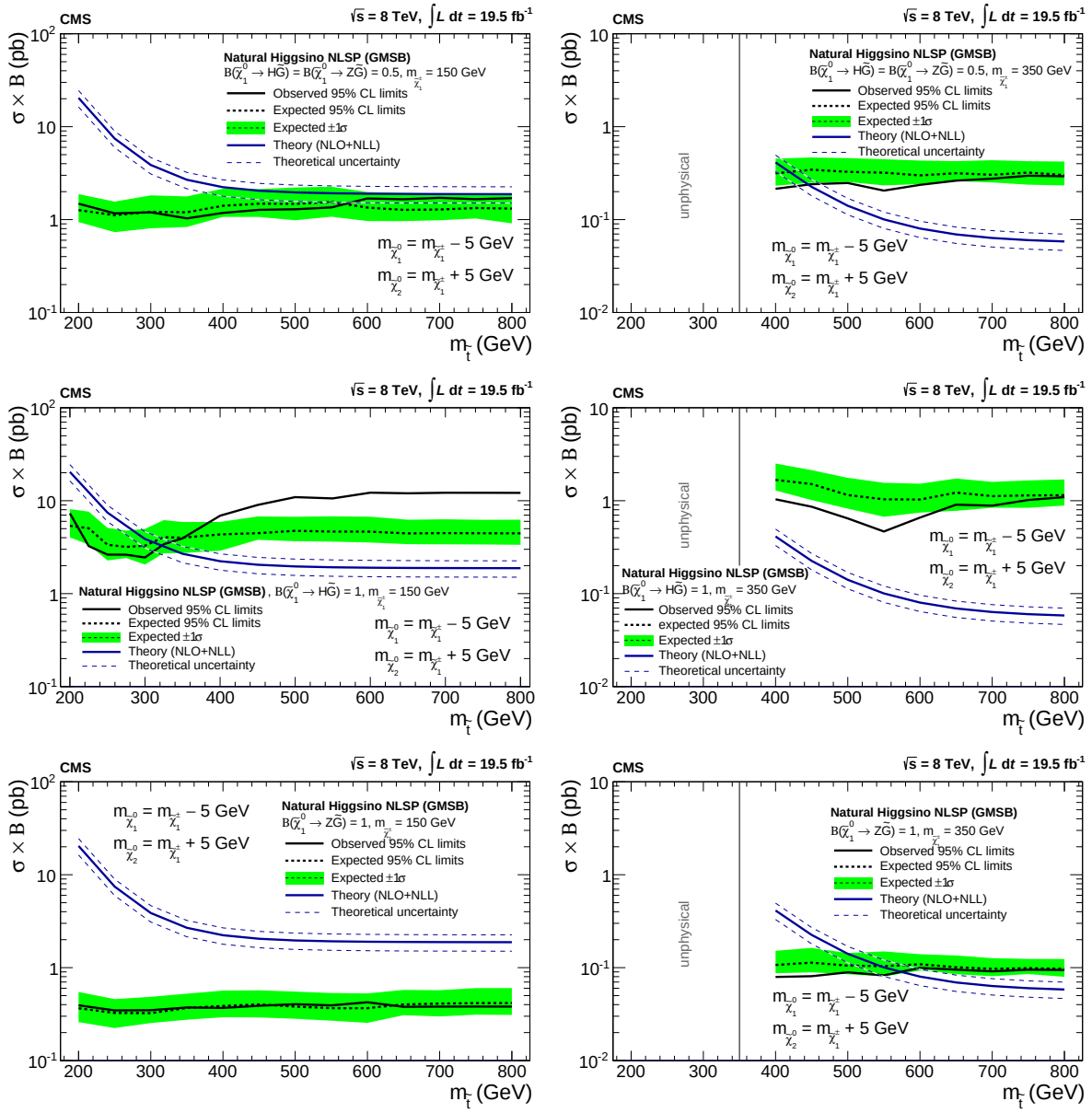

Figure 5: The 95% confidence level upper limits on cross section times branching fraction $\mathcal{B}$, for the natural higgsino NLSP scenario for $\mathcal{B}(\widetilde{\chi}_1^0 \to \mathrm{H}\widetilde{\mathrm{G}}) = \mathcal{B}(\widetilde{\chi}_1^0 \to \mathrm{Z}\widetilde{\mathrm{G}}) = 0.5$ (top), $\mathcal{B}(\widetilde{\chi}_1^0 \to \mathrm{H}\widetilde{\mathrm{G}}) = 1.0$ (middle), and $\mathcal{B}(\widetilde{\chi}_1^0 \to \mathrm{Z}\widetilde{\mathrm{G}}) = 1.0$ (bottom). The charged higgsino mass is fixed at 150 GeV (left) and 350 GeV (right). The region to the left of the vertical line on the right plots is unphysical and limited by the charged higgsino mass.

mass spectrum are shown in Fig. 7. The $\widetilde{\chi}_1^0$ neutralino is taken to be a bino, the superpartner of the B gauge boson. The bino decays to a lepton and the NLSP, while the NLSP decays to the gravitino LSP and an additional lepton. Depending on the mass spectrum, the events can have large H_{T}. Channels with no tagged b jets and off-Z OSSF pairs exhibit the largest sensitivity for this scenario.

Beyond production through squarks and gluinos, production through chargino-neutralino or right-handed slepton pairs is possible. The decay of each parent eventually leads to a bino $\widetilde{\chi}_1^0$, which decays as shown in Fig. 7, leading to a final state with multileptons and $E_{\mathrm{T}}^{\mathrm{miss}}$ as for the strong-production process. The relative importance of the strong- and weak- production

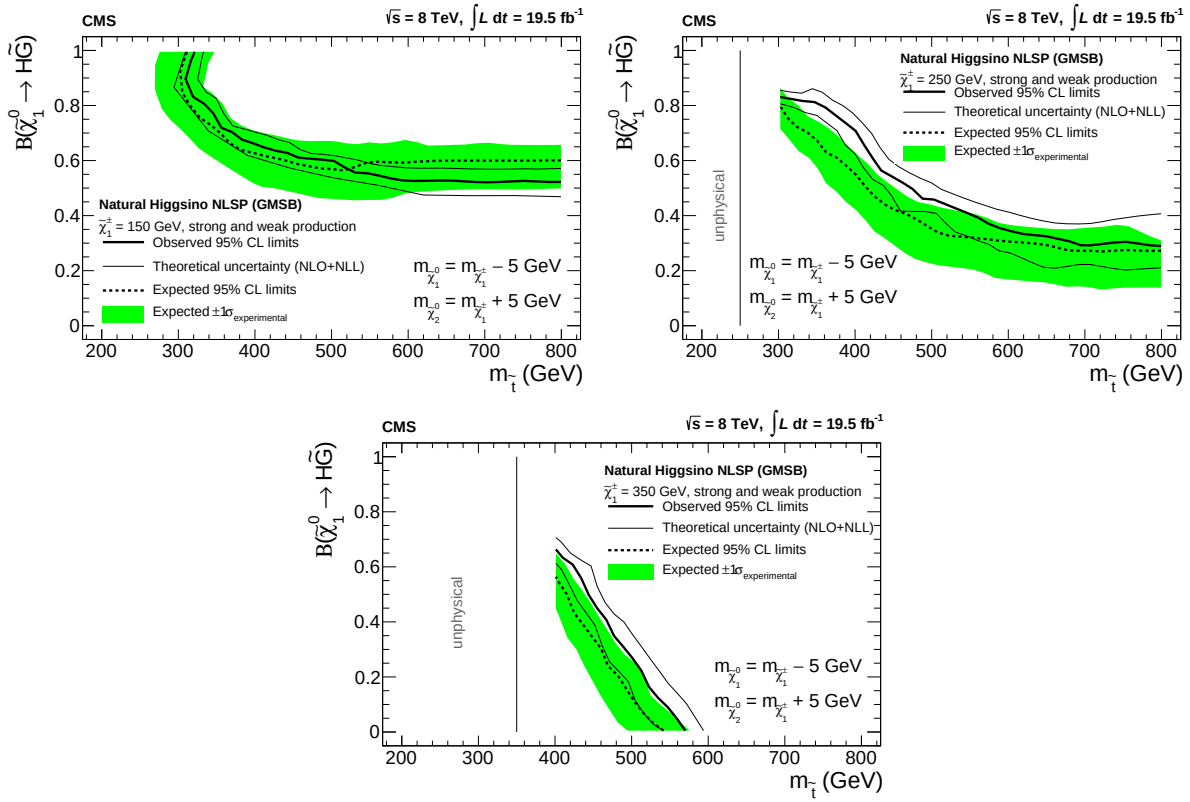

Figure 6: The 95% confidence level upper limits on the branching fraction $\mathcal{B}(\tilde{\chi}_1^0 \to \mathrm{H}\tilde{\mathrm{G}})$ for the natural higgsino NLSP scenario with fixed charged higgsino mass of 150 GeV (upper left), 250 GeV (upper right), and 350 GeV (bottom) assuming $\mathcal{B}(\tilde{\chi}_1^0 \to \mathrm{H}\tilde{\mathrm{G}}) + \mathcal{B}(\tilde{\chi}_1^0 \to \mathrm{Z}\tilde{\mathrm{G}}) = 1.0$. The region to the left of the vertical line on the right plots is unphysical and limited by the charged higgsino mass.

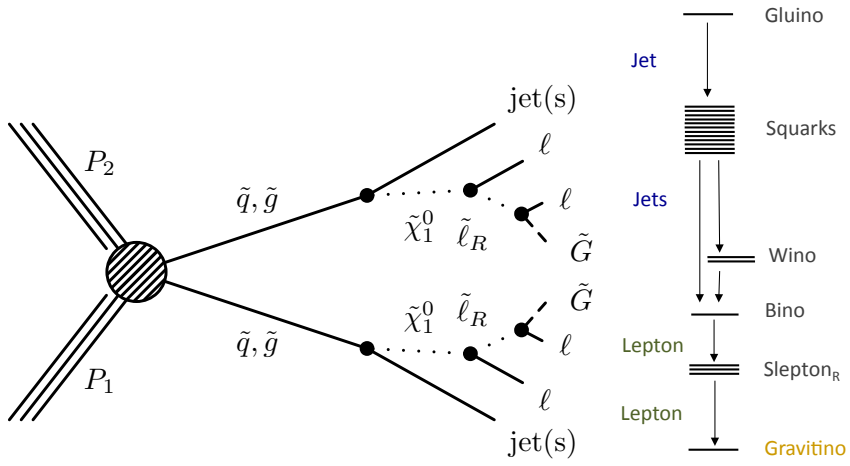

Figure 7: Event diagram and a schematic superpartner mass spectrum for the GMSB slepton co-NLSP scenario.

mechanisms depends on the values of the superpartner masses.

Signal events for the slepton co-NLSP scenario are generated using the PYTHIA generator. The superpartner mass spectrum is parametrized in terms of the masses of the $\tilde{\chi}_1^{\pm}$ chargino and the gluino. The remaining superpartner masses are chosen to be $m_{\tilde{\ell}_R} = 0.3 m_{\tilde{\chi}_1^{\pm}}$, $m_{\tilde{\chi}_1^0} = 0.5 m_{\tilde{\chi}_1^{\pm}}$,

$m_{\tilde{\ell}_L} = 0.8m_{\tilde{\chi}_1^\pm}$, and $m_{\tilde{q}} = 0.8m_{\tilde{g}}$, with no mixing of the left- and right-handed slepton and squark components, and with the higgsino masses so large that their contributions are negligible. The cross sections are calculated at NLO using K-factors from PROSPINO [48] and are assigned a 30% theoretical uncertainty, taking into account cross section, scale, and PDF uncertainties.

The 95% CL exclusions limits for the slepton co-NLSP scenario are shown in Fig. 8 (left) as a function of the gluino and chargino masses. In the region dominated by strong superpartner production, the exclusion curve asymptotically approaches a horizontal plateau, while it tends towards a vertical line in the region dominated by weak superpartner production.

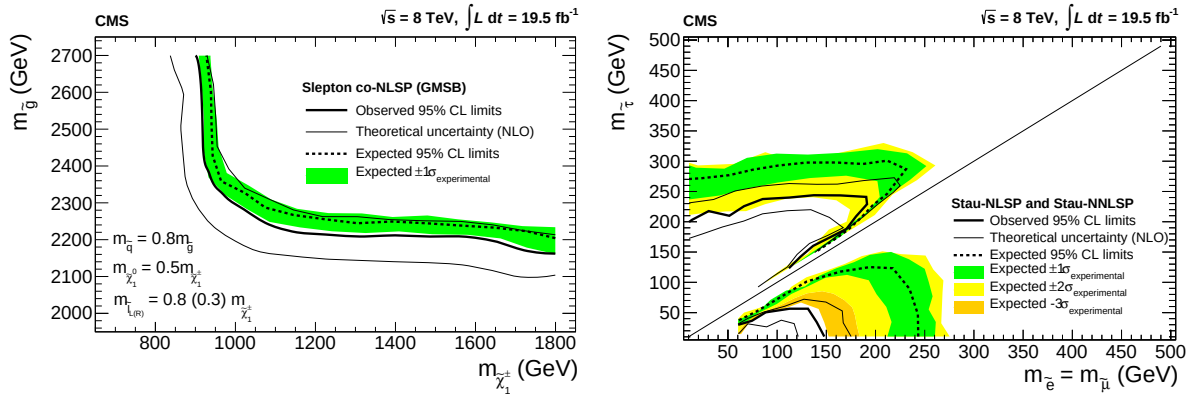

Figure 8: The 95% confidence level upper limits for the slepton co-NLSP model in the gluino versus chargino mass plane (left) and for the stau-(N)NLSP scenarios in the stau versus degenerate-smuon and -selectron mass plane (right). The region to the left and below the contours is excluded.

8.3 The stau-(N)NLSP scenario

In the stau-NLSP scenario, the right-handed stau lepton is the NLSP. This scenario arises for moderate to large values of the MSSM parameter $\tan\beta$ [4, 5]. Mass-degenerate right-handed selectrons and smuons decay to the stau through the three-body processes $\tilde{e}_R \to \tilde{\tau}_R \tau e$ and $\tilde{\mu}_R \to \tilde{\tau}_R \tau \mu$. The stau decays as $\tilde{\tau}_R \to \tilde{G}\tau$. Pair production of selectrons or smuons leads to a multilepton final state dominated by τ leptons. A diagram and schematic mass spectrum are shown in Fig. 9.

Besides the stau-NLSP scenario, we also consider the stau-NNLSP scenario in which mass-degenerate right-handed selectrons and smuons are co-NLSPs, while the right-handed stau is the next-to-next-to-lightest SUSY particle (NNLSP). The process proceeds via electroweak pair production of staus. The staus decay to the NLSP and a τ lepton. The NLSPs decay to a τ lepton and gravitino.

The search channels most sensitive to the stau-(N)NLSP scenarios contain τ_h leptons, no tagged b jets, off-Z OSSF pairs, and large E_T^{miss}. Signal events for the stau-(N)NLSP model are generated using PYTHIA [31]. The cross sections are normalized to NLO calculations using PROSPINO [48] and are assigned a 30% theoretical uncertainty.

The 95% CL exclusion limits for the stau-(N)NLSP scenario are shown in Fig. 8 (bottom). When the mass difference between the stau and the other sleptons is small, the leptons are soft. This results in low signal efficiency, which causes the exclusion contour to become nearly parallel to the diagonal for points near the diagonal. The difference between the expected and observed limits in the region below the diagonal is driven by the excesses observed between the data

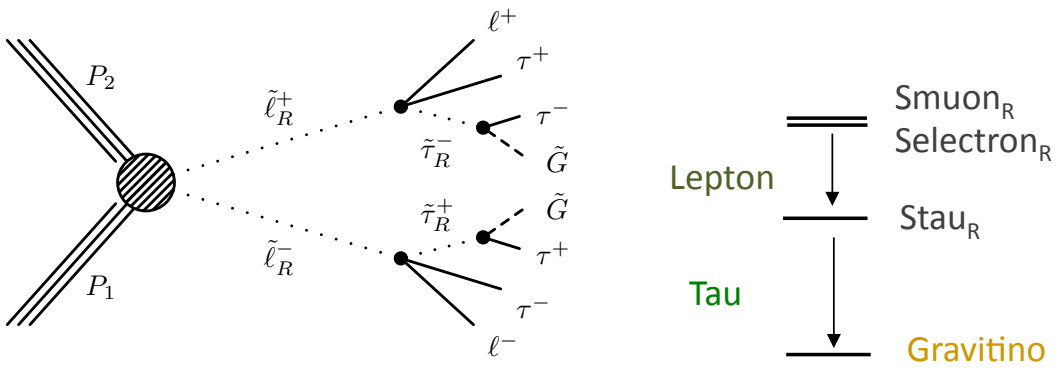

Figure 9: Event diagram and a schematic superpartner mass spectrum for the GMSB stau-(N)NLSP scenario.

and SM estimates in the four-or-more lepton, OSSF1, off-Z, τ_h channels without b jets, noted in Section 7.

8.4 Third-generation SMS scenario T1tttt

In the T1tttt simplified model spectra (SMS) scenario [46, 49], pair-produced gluinos each decay to a top quark and a virtual top squark. The virtual top squark decays to a top quark and the LSP, where the LSP is the lightest neutralino. Thus each gluino undergoes an effective three-body decay to two top quarks and the LSP, yielding four top quarks in the final state. Each top quark can potentially yield a b jet and a leptonically decaying W boson, leading to a multilepton final state with b jets and E_T^{miss}. Because of the large number of jets, the H_T value can be quite large. An event diagram and schematic mass spectrum are shown in Fig. 10.

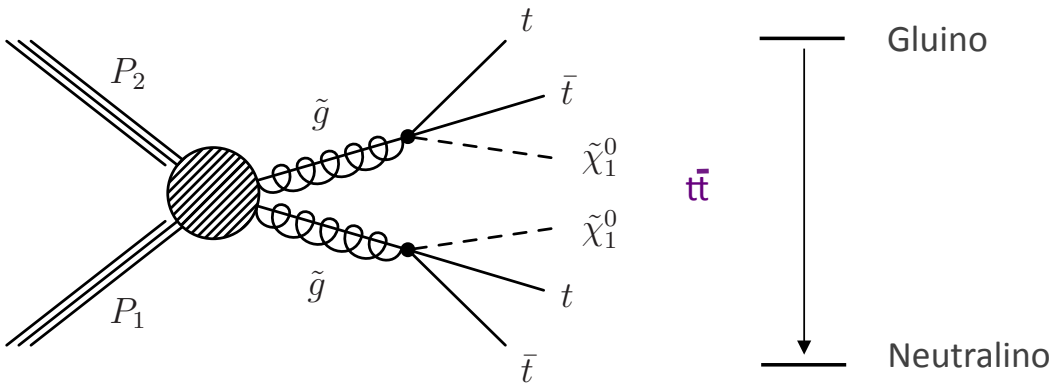

Figure 10: Event diagram and a schematic superpartner mass spectrum for the SMS T1tttt scenario.

The presence of four top quarks in the final state results in four b quarks and four W bosons. The W-boson decays can produce up to four leptons with large E_T^{miss}. The SM background is significantly reduced by requiring the presence of a b jet. This requirement represents an improvement with respect to our analysis of the 7 TeV data [11]. Ours is the first study of the T1tttt scenario in the multilepton channel.

Signal events for the T1tttt scenario are generated using MADGRAPH. The cross sections are calculated at the NLO plus next-to-leading-logarithm (NLL) level [47, 50–53] with uncertainties that vary between 23% and 27% [54].

The 95% CL exclusion limits in the gluino versus LSP mass plane are shown in Fig. 11 (left). We exclude gluinos with mass values below 1 TeV over much of this plane.

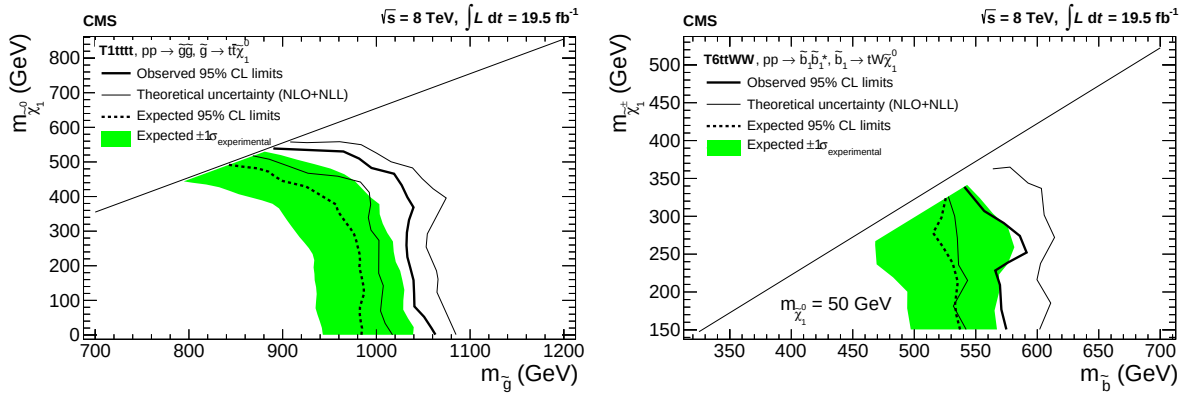

Figure 11: 95% confidence level upper limits for the T1tttt scenario in the LSP versus gluino mass plane (left) and for the T6ttWW scenario in the chargino versus bottom-squark mass plane (right) are shown. Masses to the left and below the contours are excluded.

8.5 Third-generation SMS scenario T6ttWW

In the T6ttWW SMS scenario, we search for SUSY signals with direct bottom-squark pair production [55]. An event diagram and schematic mass spectrum are shown in Fig. 12. The bottom squark decays as $\tilde{b} \to t\tilde{\chi}_1^-$, while the chargino decays as $\tilde{\chi}_1^- \to W^-\tilde{\chi}_1^0$. This scenario populates channels with tagged b jets.

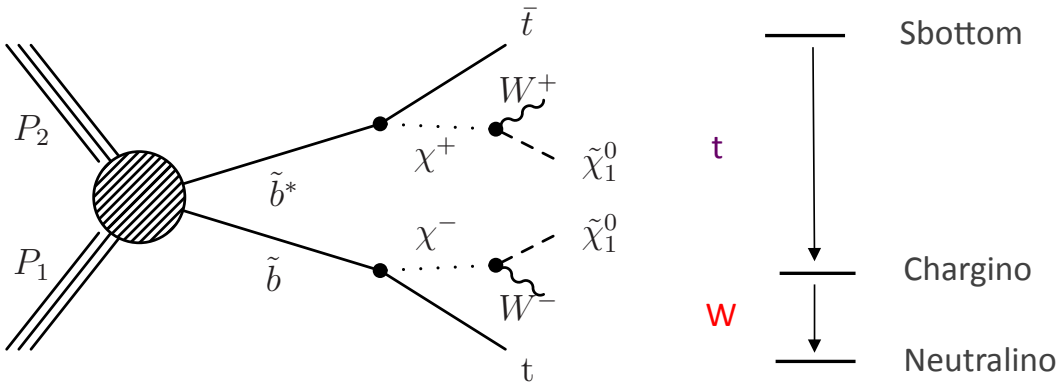

Figure 12: Event diagram and a schematic superpartner mass spectrum for the SMS T6ttWW scenario.

For simplicity, we consider on-shell charginos. The W boson from the chargino decay can be either on- or off-shell. Signal events are generated using MADGRAPH with normalization of the cross section performed to NLO+NLL [47, 50–53]. The uncertainty of the cross section calculation is 30% [54].

Figure 11 (bottom) shows the exclusion limits for the T6ttWW scenario in the chargino versus bottom-squark mass plane. The mass of the $\tilde{\chi}_1^0$ is assumed to be 50 GeV. We exclude bottom squarks with mass values less than 550 GeV. This result complements our study of this same scenario performed using same-sign dilepton events and obtains similar conclusions [56].

9 Rare decay $t \to cH$

Beyond the SUSY scenarios examined in Section 8, we interpret our results in the context of the flavor-changing decay of a top quark to a Higgs boson and a charm quark. Although not forbidden in the SM, the SM branching fraction is predicted to be extremely small (10^{-13}–10^{-15} [9, 10]), due to suppression both by the Glashow–Iliopoulos–Maiani mechanism [57] and by the Cabibbo–Kobayashi–Maskawa quark-mixing matrix [58] factor. Observation of the $t \to cH$ transition can therefore provide evidence for BSM physics, i.e., for non-SM particles produced virtually in loops. In this sense the $t \to cH$ transition plays a complementary role to SUSY searches compared to the direct superpartner production scenarios considered in Section 8.

In addition, the $t \to cH$ decay directly probes the flavor-violating couplings of the Higgs boson to the top quark. Since up-type quark-flavor violation is less constrained than down-type quark-flavor violation [59], exploration of this issue is of general interest.

The production of a $t\bar{t}$ pair followed by the decay of one top quark to a cH state and the other to a bW state can yield a multilepton signature, especially if the Higgs boson decays through one of the following channels:

- $H \to WW^* \to \ell\nu\ell\nu$,
- $H \to \tau\tau$, or
- $H \to ZZ^* \to jj\ell\ell, \nu\nu\ell\ell, \ell\ell\ell\ell$,

where j refers to a jet. If the $t \to bW$ decay also produces a lepton, there can be up to five leptons in an event.

To simulate signal events, we generate a $t\bar{t}$ sample in which one top quark decays to cH and the other to bW. We assume $m_H = 126\,\text{GeV}$ [60] and that the Higgs boson has SM branching fractions. We only consider the decay modes listed above because the contributions of other Higgs boson decay modes to the multilepton final state are found to be negligible. Signal events are generated using MADGRAPH, with normalization performed at the next-to-next-to-leading order [61].

The signal events predominantly populate channels with three leptons, a tagged b jet, no τ_h-lepton candidate, and an OSSF off-Z pair or no OSSF pair. The most sensitive channels are listed in Table 4. The main source of SM background arises from $t\bar{t}$ production. The observed numbers of events are seen to be in agreement with the SM expectations to within the uncertainties.

Using the same limit-setting procedure as in Section 8, we obtain a 95% CL upper limit on the branching fraction of $\mathcal{B}(t \to cH) < 1.3\%$. The measured branching fraction is $(1.2^{+0.5}_{-0.3})\%$. The uncertainties include both the statistical and systematic terms. The observed limit corresponds to a bound on the left- and right-handed top-charm flavor-violating Higgs Yukawa couplings, λ^H_{tc} and λ^H_{ct}, respectively, of $\sqrt{|\lambda^H_{tc}|^2 + |\lambda^H_{ct}|^2} < 0.21$. This result represents a significant improvement compared with the inferred result $\sqrt{|\lambda^H_{tc}|^2 + |\lambda^H_{ct}|^2} < 0.31$ from Ref. [9], which is based on our 7 TeV results [11]. Table 5 present upper limits from individual Higgs boson decay modes. All other decay modes are ignored when calculating these limits. It is seen that the $H \to WW^* \to \ell\nu\ell\nu$ mode dominates the overall result.

Table 4: The ten most sensitive signal regions for the $t \to cH$ process, along with the number of observed (Obs.), background (Exp.), and expected signal (Sig.) events, assuming $\mathcal{B}(t \to cH) = 1\%$, ordered by sensitivity. All signal regions shown have exactly three selected leptons. The results are binned in E_T^{miss}, H_T, number of tagged b jets or τ_h candidates, and, if an OSSF pair is present, its invariant mass with respect to the Z-boson mass window.

OSSF pair	N_{τ_h}	E_T^{miss} (GeV)	H_T (GeV)	N_b	Obs.	Exp.	Sig.
Below-Z	0	50–100	0–200	$\geq$1	48	48 ± 23	9.5 ± 2.3
—	0	50–100	0–200	$\geq$1	29	26 ± 13	5.9 ± 1.3
Below-Z	0	0–50	0–200	$\geq$1	34	42 ± 11	5.9 ± 1.2
—	0	0–50	0–200	$\geq$1	29	23 ± 10	4.3 ± 1.1
Below-Z	0	50–100	> 200	$\geq$1	10	9.9 ± 3.7	3.0 ± 1.1
Below-Z	0	0–50	> 200	$\geq$1	5	10 ± 2.5	2.8 ± 0.8
Below-Z	0	50–100	0–200	0	142	125 ± 27	9.7 ± 2.1
—	1	0–50	0–200	$\geq$1	237	240 ± 113	13.1 ± 2.6
—	0	50–100	0–200	0	35	38 ± 15	4.3 ± 1.1
Above-Z	0	0–50	0–200	$\geq$1	17	18 ± 6.7	2.8 ± 0.8

Table 5: Comparison of the observed and median expected 95% CL upper limits on $\mathcal{B}(t \to cH)$ from individual Higgs boson decay modes, along with their one standard deviation (σ) uncertainties. The uncertainties include both statistical and systematic terms.

Higgs boson decay mode		Upper limits on $\mathcal{B}(t \to cH)$		
		Obs.	Exp.	1σ range
$\mathcal{B}(H \to WW^*)$	$= 23.1\%$	1.6 %	1.6%	(1.0–2.2)%
$\mathcal{B}(H \to \tau\tau)$	$= 6.2\%$	7.01%	5.0 %	(3.5–7.7)%
$\mathcal{B}(H \to ZZ^*)$	$= 2.9\%$	5.3%	4.11%	(2.9–6.5)%
Combined		1.3%	1.2%	(0.9–1.7)%

10 Summary

We have performed a search for physics beyond the standard model based on events with three or more leptons, where one of these leptons can be a hadronically decaying τ lepton. We search in channels with e^+e^- or $\mu^+\mu^-$ pairs that are either consistent or inconsistent with Z boson decay, in channels without such a pair, in channels with or without a hadronically decaying τ-lepton candidate, in channels with and without a tagged bottom-quark jet, in events with and without a large level of jet activity (measured with the scalar sum of jet p_T values), and in different bins of missing transverse energy. We find no significant excesses compared to the expectations from standard model processes. The search is performed separately for events with exactly three leptons and with four or more leptons.

We examine a broad class of supersymmetric scenarios that, taken together, populate a broad spectrum of multilepton final states. Compared to previous results, we probe new regions of the parameter space for the natural higgsino next-to-lightest supersymmetric particle (NLSP), slepton co-NLSP, and stau-(N)NLSP scenarios, where (N)NLSP denotes the (next-to-)next-to-lightest-supersymmetric particle. In addition, we investigate scenarios with gluino pair production followed by gluino decay to a top-antitop pair and the lightest supersymmetric particle, and direct bottom-squark pair production. Cross section upper limits at 95% confidence level are presented for all these scenarios.

We further explore rare transitions of the top quark to a charm quark and a Higgs boson, $t \to cH$. We set a 95% confidence level upper limit of 1.3% on the branching fraction of this decay,

which corresponds to an upper bound $\sqrt{|\lambda^{H}_{tc}|^2 + |\lambda^{H}_{ct}|^2} < 0.21$ on the flavor-violating couplings of a Higgs boson to a tc quark combination.

Acknowledgements

We congratulate our colleagues in the CERN accelerator departments for the excellent performance of the LHC and thank the technical and administrative staffs at CERN and at other CMS institutes for their contributions to the success of the CMS effort. In addition, we gratefully acknowledge the computing centres and personnel of the Worldwide LHC Computing Grid for delivering so effectively the computing infrastructure essential to our analyses. Finally, we acknowledge the enduring support for the construction and operation of the LHC and the CMS detector provided by the following funding agencies: the Austrian Federal Ministry of Science, Research and Economy and the Austrian Science Fund; the Belgian Fonds de la Recherche Scientifique, and Fonds voor Wetenschappelijk Onderzoek; the Brazilian Funding Agencies (CNPq, CAPES, FAPERJ, and FAPESP); the Bulgarian Ministry of Education and Science; CERN; the Chinese Academy of Sciences, Ministry of Science and Technology, and National Natural Science Foundation of China; the Colombian Funding Agency (COLCIENCIAS); the Croatian Ministry of Science, Education and Sport, and the Croatian Science Foundation; the Research Promotion Foundation, Cyprus; the Ministry of Education and Research, Recurrent financing contract SF0690030s09 and European Regional Development Fund, Estonia; the Academy of Finland, Finnish Ministry of Education and Culture, and Helsinki Institute of Physics; the Institut National de Physique Nucléaire et de Physique des Particules / CNRS, and Commissariat à l'Énergie Atomique et aux Énergies Alternatives / CEA, France; the Bundesministerium für Bildung und Forschung, Deutsche Forschungsgemeinschaft, and Helmholtz-Gemeinschaft Deutscher Forschungszentren, Germany; the General Secretariat for Research and Technology, Greece; the National Scientific Research Foundation, and National Innovation Office, Hungary; the Department of Atomic Energy and the Department of Science and Technology, India; the Institute for Studies in Theoretical Physics and Mathematics, Iran; the Science Foundation, Ireland; the Istituto Nazionale di Fisica Nucleare, Italy; the Korean Ministry of Education, Science and Technology and the World Class University program of NRF, Republic of Korea; the Lithuanian Academy of Sciences; the Ministry of Education, and University of Malaya (Malaysia); the Mexican Funding Agencies (CINVESTAV, CONACYT, SEP, and UASLP-FAI); the Ministry of Business, Innovation and Employment, New Zealand; the Pakistan Atomic Energy Commission; the Ministry of Science and Higher Education and the National Science Centre, Poland; the Fundação para a Ciência e a Tecnologia, Portugal; JINR, Dubna; the Ministry of Education and Science of the Russian Federation, the Federal Agency of Atomic Energy of the Russian Federation, Russian Academy of Sciences, and the Russian Foundation for Basic Research; the Ministry of Education, Science and Technological Development of Serbia; the Secretaría de Estado de Investigación, Desarrollo e Innovación and Programa Consolider-Ingenio 2010, Spain; the Swiss Funding Agencies (ETH Board, ETH Zurich, PSI, SNF, UniZH, Canton Zurich, and SER); the Ministry of Science and Technology, Taipei; the Thailand Center of Excellence in Physics, the Institute for the Promotion of Teaching Science and Technology of Thailand, Special Task Force for Activating Research and the National Science and Technology Development Agency of Thailand; the Scientific and Technical Research Council of Turkey, and Turkish Atomic Energy Authority; the National Academy of Sciences of Ukraine, and State Fund for Fundamental Researches, Ukraine; the Science and Technology Facilities Council, UK; the US Department of Energy, and the US National Science Foundation.

Individuals have received support from the Marie-Curie programme and the European Re-

search Council and EPLANET (European Union); the Leventis Foundation; the A. P. Sloan Foundation; the Alexander von Humboldt Foundation; the Belgian Federal Science Policy Office; the Fonds pour la Formation à la Recherche dans l'Industrie et dans l'Agriculture (FRIA-Belgium); the Agentschap voor Innovatie door Wetenschap en Technologie (IWT-Belgium); the Ministry of Education, Youth and Sports (MEYS) of Czech Republic; the Council of Science and Industrial Research, India; the Compagnia di San Paolo (Torino); the HOMING PLUS programme of Foundation for Polish Science, cofinanced by EU, Regional Development Fund; and the Thalis and Aristeia programmes cofinanced by EU-ESF and the Greek NSRF.

References

[1] ATLAS Collaboration, "Observation of a new particle in the search for the Standard Model Higgs boson with the ATLAS detector at the LHC", *Phys. Lett. B* **716** (2012) 1, doi:10.1016/j.physletb.2012.08.020, arXiv:1207.7214.

[2] CMS Collaboration, "Observation of a new boson at a mass of 125 GeV with the CMS experiment at the LHC", *Phys. Lett. B* **716** (2012) 30, doi:10.1016/j.physletb.2012.08.021, arXiv:1207.7235.

[3] CMS Collaboration, "Observation of a new boson with mass near 125 GeV in pp collisions at $\sqrt{s}$ = 7 and 8 TeV", *JHEP* **06** (2013) 081, doi:10.1007/JHEP06(2013)081, arXiv:1303.4571.

[4] H. P. Nilles, "Supersymmetry, Supergravity and Particle Physics", *Phys. Rept.* **110** (1984) 1, doi:10.1016/0370-1573(84)90008-5.

[5] H. E. Haber and G. L. Kane, "The Search for Supersymmetry: Probing Physics Beyond the Standard Model", *Phys. Rept.* **117** (1985) 75, doi:10.1016/0370-1573(85)90051-1.

[6] W. de Boer, "Grand unified theories and supersymmetry in particle physics and cosmology", *Prog. Part. Nucl. Phys.* **33** (1994) 201, doi:10.1016/0146-6410(94)90045-0.

[7] G. R. Farrar and P. Fayet, "Phenomenology of the production, decay, and detecion of new hadronic states associated with supersymmetry", *Phys. Lett. B* **76** (1978) 575, doi:0.1016/0370-2693(78)90858-4.

[8] G. Brooijmans et al., "New Physics at the LHC. A Les Houches Report", (2010). arXiv:1005.1229.

[9] N. Craig et al., "Searching for t $\to$ cH with Multi-Leptons", *Phys. Rev. D* **86** (2012) 075002, doi:10.1103/PhysRevD.86.075002, arXiv:1207.6794v2.

[10] K.-F. Chen, W.-S. Hou, C. Kao, and M. Kohda, "When the Higgs meets the Top: Search for t $\to$ cH at the LHC", *Phys. Lett. B* **725** (2013) 378, doi:10.1016/j.physletb.2013.07.060, arXiv:1304.8037v2.

[11] CMS Collaboration, "Search for anomalous production of multilepton events in pp collisions at $\sqrt{s} = 7$ TeV", *JHEP* **06** (2012) 169, doi:10.1007/JHEP06(2012)169, arXiv:1204.5341.

[12] CMS Collaboration, "Search for top squarks in R-parity-violating supersymmetry using three or more leptons and b-tagged jets", *Phys. Rev. Lett.* **111** (2013) 221801, doi:10.1103/PhysRevLett.111.221801, arXiv:1306.6643v2.

[13] ATLAS Collaboration, "Search for R-parity-violating supersymmetry in events with four or more leptons in $\sqrt{s} = 7$ TeV pp collisions with the ATLAS detector", *JHEP* **12** (2012) 124, doi:10.1007/JHEP12(2012)124, arXiv:1210.4457.

[14] CMS Collaboration, "The CMS experiment at the CERN LHC", *JINST* **3** (2008) S08004, doi:10.1088/1748-0221/3/08/S08004.

[15] CMS Collaboration, "Commissioning of the Particle-Flow Reconstruction in Minimum-Bias and Jet Events from pp Collisions at 7 TeV", CMS Physics Analysis Summary CMS-PAS-PFT-10-002, 2010.

[16] CMS Collaboration, "Particle–Flow Event Reconstruction in CMS and Performance for Jets, Taus, and $E_{\mathrm{T}}^{\mathrm{miss}}$", CMS Physics Analysis Summary CMS-PAS-PFT-09-001, 2009.

[17] CMS Collaboration, "Electron Reconstruction and Identification at $\sqrt{s} = 7$ TeV", CMS Physics Analysis Summary CMS-PAS-EGM-10-004, 2010.

[18] CMS Collaboration, "CMS MET Performance in Events Containing Electroweak Bosons from pp Collisions at $\sqrt{s} = 7$ TeV", CMS Physics Analysis Summary CMS-PAS-JME-10-005, 2010.

[19] CMS Collaboration, "Missing transverse energy performance of the CMS detector", *JINST* **6** (2011) P09001, doi:10.1088/1748-0221/6/09/P09001.

[20] M. Cacciari, G. P. Salam, and G. Soyez, "The anti-k_{T} jet clustering algorithm", *JHEP* **04** (2008) 063, doi:10.1088/1126-6708/2008/04/063, arXiv:0802.1189v2.

[21] M. Cacciari, G. P. Salam, and G. Soyez, "FastJet User Manual", *Eur. Phys. J. C* **72** (2012) 1896, doi:10.1140/epjc/s10052-012-1896-2, arXiv:1111.6097v1.

[22] CMS Collaboration, "Determination of jet energy calibration and transverse momentum resolution in CMS", *JINST* **6** (2011) P11002, doi:10.1088/1748-0221/6/11/P11002.

[23] M. Cacciari and G. P. Salam, "Pileup subtraction using jet areas", *Phys. Lett. B* **659** (2008) 119, doi:10.1016/j.physletb.2007.09.077, arXiv:0707.1378v2.

[24] CMS Collaboration, "Identification of b-quark jets with the CMS experiment", *JINST* **8** (2013) P04013, doi:10.1088/1748-0221/8/04/P04013, arXiv:1211.4462.

[25] F. Maltoni and T. Stelzer, "MadEvent: Automatic event generation with MadGraph", *JHEP* **02** (2003) 027, doi:10.1088/1126-6708/2003/02/027, arXiv:hep-ph/0208156v1.

[26] P. M. Nadolsky et al., "Implications of CTEQ global analysis for collider observables", *Phys. Rev. D* **78** (2008) 013004, doi:10.1103/PhysRevD.78.013004, arXiv:0802.0007.

[27] GEANT4 Collaboration, "GEANT4—a simulation toolkit", *Nucl. Instrum. Meth. A* **506** (2003) 250, doi:10.1016/S0168-9002(03)01368-8.

[28] J. Campbell, R. K. Ellis, and C. Williams, "Vector boson pair production at the LHC", *JHEP* **07** (2011) 018, doi:10.1007/JHEP07(2011)018, arXiv:1105.0020.

[29] J. M. Campbell and R. K. Ellis, "$\mathrm{t\bar{t}W^{\pm}}$ production and decay at NLO", *JHEP* **07** (2012) 052, doi:10.1007/JHEP07(2012)052, arXiv:1204.5678v1.

[30] M. V. Garzelli, A. Kardos, C. G. Papadopoulos, and Z. Trocsanyi, "$t\bar{t}W^{\pm}$ and $t\bar{t}Z$ Hadroproduction at NLO accuracy in QCD with Parton Shower and Hadronization effects", *JHEP* **11** (2012) 056, doi:10.1007/JHEP11(2012)056, arXiv:1208.2665v1.

[31] T. Sjöstrand, S. Mrenna, and P. Z. Skands, "A brief introduction to PYTHIA 8.1", *Comput. Phys. Commun.* **178** (2008) 852, doi:10.1016/j.cpc.2008.01.036, arXiv:0710.3820v1.

[32] CMS Collaboration, "Fast simulation of the CMS detector", *J. Phys. Conf. Ser.* **219** (2010) 032053, doi:10.1088/1742-6596/219/3/032053.

[33] CMS Collaboration, "Search for top-squark pair production in the single-lepton final state in pp collisions at $\sqrt{s} = 8$ TeV", *Eur. Phys. J. C* **73** (2013) 2677, doi:10.1140/epjc/s10052-013-2677-2, arXiv:1308.1586v2.

[34] CMS Collaboration, "Performance of CMS muon reconstruction in pp collision events at $\sqrt{s} = 7$ TeV", *JINST* **7** (2012) P10002, doi:10.1088/1748-0221/7/10/P10002.

[35] CMS Collaboration, "Search for heavy lepton partners of neutrinos in proton-proton collisions in the context of the type III seesaw mechanism", *Phys. Lett. B* **718** (2012) 348, doi:10.1016/j.physletb.2012.10.070, arXiv:1210.1797.

[36] CMS Collaboration, "Performance of τ-lepton reconstruction and identification in CMS", *JINST* **7** (2012) P01001, doi:10.1088/1748-0221/7/01/P01001.

[37] CMS Collaboration, "CMS Luminosity Based on Pixel Cluster Counting - Summer 2013 Update", CMS Physics Analysis Summary CMS-PAS-LUM-13-001, 2013.

[38] ATLAS and CMS Collaborations, "Procedure for the LHC Higgs boson search combination in Summer 2011", Technical Report CMS-NOTE-2011-005, ATLAS/CMS, Geneva, 2011.

[39] T. Junk, "Confidence Level Computation for Combining Searches with Small Statistics", *Nucl. Instrum. Meth. A* **434** (1999) 435, doi:10.1016/S0168-9002(99)00498-2, arXiv:hep-ex/9902006.

[40] A. L. Read, "Presentation of search results: The CL(s) technique", *J. Phys. G* **28** (2002) 2693, doi:10.1088/0954-3899/28/10/313.

[41] CMS Collaboration, "Search for top squark and higgsino production using diphoton Higgs boson decays", (2013). arXiv:1312.3310v1. Submitted to Phys. Rev. Lett.

[42] K. T. Matchev and S. Thomas, "Higgs and Z-boson signatures of supersymmetry", *Phys. Rev. D* **62** (2000) 077702, doi:10.1103/PhysRevD.62.077702, arXiv:hep-ph/9908482.

[43] S. Dimopoulos, S. D. Thomas, and J. D. Wells, "Implications of low energy supersymmetry breaking at the Fermilab Tevatron", *Phys. Rev. D* **54** (1996) 3283, doi:10.1103/PhysRevD.54.3283, arXiv:hep-ph/9604452v3.

[44] SUSY Working Group Collaboration, "Low scale and gauge mediated supersymmetry breaking at the Fermilab Tevatron Run II", (2000). arXiv:hep-ph/0008070v2.

[45] J. T. Ruderman and D. Shih, "Slepton co-NLSPs at the Tevatron", *JHEP* **11** (2010) 046, doi:10.1007/JHEP11(2010)046, arXiv:1009.1665.

[46] LHC New Physics Working Group Collaboration, "Simplified Models for LHC New Physics Searches", *J. Phys. G* **39** (2012) 105005, doi:10.1088/0954-3899/39/10/105005, arXiv:1105.2838.

[47] W. Beenakker, R. Hopker, M. Spira, and P. M. Zerwas, "Squark and gluino production at hadron colliders", *Nucl. Phys. B* **492** (1997) 51, doi:10.1016/S0550-3213(97)80027-2, arXiv:hep-ph/9610490v1.

[48] W. Beenakker, R. Hopker, and M. Spira, "PROSPINO: A program for the production of supersymmetric particles in next-to-leading order QCD", 1996, arXiv:hep-ph/9611232v1.

[49] R. Essig, E. Izaguirre, J. Kaplan, and J. G. Wacker, "Heavy Flavor Simplified Models at the LHC", *JHEP* **01** (2012) 074, doi:10.1007/JHEP01(2012)074, arXiv:1110.6443v1.

[50] A. Kulesza and L. Motyka, "Threshold resummation for squark-antisquark and gluino-pair production at the LHC", *Phys. Rev. Lett.* **102** (2009) 111802, doi:10.1103/PhysRevLett.102.111802, arXiv:0807.2405v1.

[51] A. Kulesza and L. Motyka, "Soft gluon resummation for the production of gluino-gluino and squark-antisquark pairs at the LHC", *Phys. Rev. D* **80** (2009) 095004, doi:10.1103/PhysRevD.80.095004, arXiv:0905.4749v1.

[52] W. Beenakker et al., "Soft-gluon resummation for squark and gluino hadroproduction", *JHEP* **12** (2009) 041, doi:10.1088/1126-6708/2009/12/041, arXiv:0909.4418v1.

[53] W. Beenakker et al., "Squark and gluino hadroproduction", *Int. J. Mod. Phys. A* **26** (2011) 2637, doi:10.1142/S0217751X11053560, arXiv:1105.1110v1.

[54] M. Krämer et al., "Supersymmetry production cross sections in pp collisions at $\sqrt{s} = 7$ TeV", (2012). arXiv:1206.2892v1.

[55] H. M. Lee, V. Sanz, and M. Trott, "Hitting sbottom in natural SUSY", *JHEP* **05** (2012) 139, doi:10.1007/JHEP05(2012)139, arXiv:1204.0802.

[56] CMS Collaboration, "Search for new physics in events with same-sign dileptons and jets in pp collisions at $\sqrt{s} = 8$ TeV", *JHEP* **01** (2013) 163, doi:10.1007/JHEP01(2014)163.

[57] S. L. Glashow, J. Iliopoulos, and L. Maiani, "Weak Interactions with Lepton-Hadron Symmetry", *Phys. Rev. D* **2** (1970) 1285, doi:10.1103/PhysRevD.2.1285.

[58] M. Kobayashi and T. Maskawa, "CP Violation in the Renormalizable Theory of Weak Interaction", *Prog. Theor. Phys.* **49** (1973) 652, doi:10.1143/PTP.49.652.

[59] M. Antonelli et al., "Flavor physics in the quark sector", *Phys. Rept.* **494** (2010) 197, doi:10.1016/j.physrep.2010.05.003, arXiv:0907.5386v2.

[60] CMS Collaboration, "Measurement of the properties of a Higgs boson in the four-lepton final state", (2013). arXiv:1312.5353v1. Submitted to Phys. Rev. D.

[61] M. Czakon, P. Fiedler, and A. Mitov, "The total top quark pair production cross-section at hadron colliders through $O(\alpha_S^4)$", *Phys. Rev. Lett.* **110** (2013) 252004, doi:10.1103/PhysRevLett.110.252004, arXiv:1303.6254.

A The CMS Collaboration

Yerevan Physics Institute, Yerevan, Armenia
S. Chatrchyan, V. Khachatryan, A.M. Sirunyan, A. Tumasyan

Institut für Hochenergiephysik der OeAW, Wien, Austria
W. Adam, T. Bergauer, M. Dragicevic, J. Erö, C. Fabjan[1], M. Friedl, R. Frühwirth[1], V.M. Ghete, C. Hartl, N. Hörmann, J. Hrubec, M. Jeitler[1], W. Kiesenhofer, V. Knünz, M. Krammer[1], I. Krätschmer, D. Liko, I. Mikulec, D. Rabady[2], B. Rahbaran, H. Rohringer, R. Schöfbeck, J. Strauss, A. Taurok, W. Treberer-Treberspurg, W. Waltenberger, C.-E. Wulz[1]

National Centre for Particle and High Energy Physics, Minsk, Belarus
V. Mossolov, N. Shumeiko, J. Suarez Gonzalez

Universiteit Antwerpen, Antwerpen, Belgium
S. Alderweireldt, M. Bansal, S. Bansal, T. Cornelis, E.A. De Wolf, X. Janssen, A. Knutsson, S. Luyckx, S. Ochesanu, B. Roland, R. Rougny, H. Van Haevermaet, P. Van Mechelen, N. Van Remortel, A. Van Spilbeeck

Vrije Universiteit Brussel, Brussel, Belgium
F. Blekman, S. Blyweert, J. D'Hondt, N. Heracleous, A. Kalogeropoulos, J. Keaveney, T.J. Kim, S. Lowette, M. Maes, A. Olbrechts, D. Strom, S. Tavernier, W. Van Doninck, P. Van Mulders, G.P. Van Onsem, I. Villella

Université Libre de Bruxelles, Bruxelles, Belgium
C. Caillol, B. Clerbaux, G. De Lentdecker, L. Favart, A.P.R. Gay, A. Léonard, P.E. Marage, A. Mohammadi, L. Perniè, T. Reis, T. Seva, L. Thomas, C. Vander Velde, P. Vanlaer, J. Wang

Ghent University, Ghent, Belgium
V. Adler, K. Beernaert, L. Benucci, A. Cimmino, S. Costantini, S. Crucy, S. Dildick, G. Garcia, B. Klein, J. Lellouch, J. Mccartin, A.A. Ocampo Rios, D. Ryckbosch, S. Salva Diblen, M. Sigamani, N. Strobbe, F. Thyssen, M. Tytgat, S. Walsh, E. Yazgan, N. Zaganidis

Université Catholique de Louvain, Louvain-la-Neuve, Belgium
S. Basegmez, C. Beluffi[3], G. Bruno, R. Castello, A. Caudron, L. Ceard, G.G. Da Silveira, C. Delaere, T. du Pree, D. Favart, L. Forthomme, A. Giammanco[4], J. Hollar, P. Jez, M. Komm, V. Lemaitre, J. Liao, O. Militaru, C. Nuttens, D. Pagano, A. Pin, K. Piotrzkowski, A. Popov[5], L. Quertenmont, M. Selvaggi, M. Vidal Marono, J.M. Vizan Garcia

Université de Mons, Mons, Belgium
N. Beliy, T. Caebergs, E. Daubie, G.H. Hammad

Centro Brasileiro de Pesquisas Fisicas, Rio de Janeiro, Brazil
G.A. Alves, M. Correa Martins Junior, T. Dos Reis Martins, M.E. Pol, M.H.G. Souza

Universidade do Estado do Rio de Janeiro, Rio de Janeiro, Brazil
W.L. Aldá Júnior, W. Carvalho, J. Chinellato[6], A. Custódio, E.M. Da Costa, D. De Jesus Damiao, C. De Oliveira Martins, S. Fonseca De Souza, H. Malbouisson, M. Malek, D. Matos Figueiredo, L. Mundim, H. Nogima, W.L. Prado Da Silva, J. Santaolalla, A. Santoro, A. Sznajder, E.J. Tonelli Manganote[6], A. Vilela Pereira

Universidade Estadual Paulista [a], Universidade Federal do ABC [b], São Paulo, Brazil
C.A. Bernardes[b], F.A. Dias[a,7], T.R. Fernandez Perez Tomei[a], E.M. Gregores[b], P.G. Mercadante[b], S.F. Novaes[a], Sandra S. Padula[a]

Institute for Nuclear Research and Nuclear Energy, Sofia, Bulgaria
V. Genchev[2], P. Iaydjiev[2], A. Marinov, S. Piperov, M. Rodozov, G. Sultanov, M. Vutova

University of Sofia, Sofia, Bulgaria
A. Dimitrov, I. Glushkov, R. Hadjiiska, V. Kozhuharov, L. Litov, B. Pavlov, P. Petkov

Institute of High Energy Physics, Beijing, China
J.G. Bian, G.M. Chen, H.S. Chen, M. Chen, R. Du, C.H. Jiang, D. Liang, S. Liang, X. Meng, R. Plestina[8], J. Tao, X. Wang, Z. Wang

State Key Laboratory of Nuclear Physics and Technology, Peking University, Beijing, China
C. Asawatangtrakuldee, Y. Ban, Y. Guo, Q. Li, W. Li, S. Liu, Y. Mao, S.J. Qian, D. Wang, L. Zhang, W. Zou

Universidad de Los Andes, Bogota, Colombia
C. Avila, L.F. Chaparro Sierra, C. Florez, J.P. Gomez, B. Gomez Moreno, J.C. Sanabria

Technical University of Split, Split, Croatia
N. Godinovic, D. Lelas, D. Polic, I. Puljak

University of Split, Split, Croatia
Z. Antunovic, M. Kovac

Institute Rudjer Boskovic, Zagreb, Croatia
V. Brigljevic, K. Kadija, J. Luetic, D. Mekterovic, S. Morovic, L. Sudic

University of Cyprus, Nicosia, Cyprus
A. Attikis, G. Mavromanolakis, J. Mousa, C. Nicolaou, F. Ptochos, P.A. Razis

Charles University, Prague, Czech Republic
M. Finger, M. Finger Jr.

Academy of Scientific Research and Technology of the Arab Republic of Egypt, Egyptian Network of High Energy Physics, Cairo, Egypt
Y. Assran[9], S. Elgammal[10], A. Ellithi Kamel[11], M.A. Mahmoud[12], A. Mahrous[13], A. Radi[10,14]

National Institute of Chemical Physics and Biophysics, Tallinn, Estonia
M. Kadastik, M. Müntel, M. Murumaa, M. Raidal, A. Tiko

Department of Physics, University of Helsinki, Helsinki, Finland
P. Eerola, G. Fedi, M. Voutilainen

Helsinki Institute of Physics, Helsinki, Finland
J. Härkönen, V. Karimäki, R. Kinnunen, M.J. Kortelainen, T. Lampén, K. Lassila-Perini, S. Lehti, T. Lindén, P. Luukka, T. Mäenpää, T. Peltola, E. Tuominen, J. Tuominiemi, E. Tuovinen, L. Wendland

Lappeenranta University of Technology, Lappeenranta, Finland
T. Tuuva

DSM/IRFU, CEA/Saclay, Gif-sur-Yvette, France
M. Besancon, F. Couderc, M. Dejardin, D. Denegri, B. Fabbro, J.L. Faure, F. Ferri, S. Ganjour, A. Givernaud, P. Gras, G. Hamel de Monchenault, P. Jarry, E. Locci, J. Malcles, A. Nayak, J. Rander, A. Rosowsky, M. Titov

Laboratoire Leprince-Ringuet, Ecole Polytechnique, IN2P3-CNRS, Palaiseau, France
S. Baffioni, F. Beaudette, P. Busson, C. Charlot, N. Daci, T. Dahms, M. Dalchenko, L. Dobrzynski,

N. Filipovic, A. Florent, R. Granier de Cassagnac, L. Mastrolorenzo, P. Miné, C. Mironov, I.N. Naranjo, M. Nguyen, C. Ochando, P. Paganini, D. Sabes, R. Salerno, J.B. Sauvan, Y. Sirois, C. Veelken, Y. Yilmaz, A. Zabi

Institut Pluridisciplinaire Hubert Curien, Université de Strasbourg, Université de Haute Alsace Mulhouse, CNRS/IN2P3, Strasbourg, France
J.-L. Agram[15], J. Andrea, D. Bloch, J.-M. Brom, E.C. Chabert, C. Collard, E. Conte[15], F. Drouhin[15], J.-C. Fontaine[15], D. Gelé, U. Goerlach, C. Goetzmann, P. Juillot, A.-C. Le Bihan, P. Van Hove

Centre de Calcul de l'Institut National de Physique Nucleaire et de Physique des Particules, CNRS/IN2P3, Villeurbanne, France
S. Gadrat

Université de Lyon, Université Claude Bernard Lyon 1, CNRS-IN2P3, Institut de Physique Nucléaire de Lyon, Villeurbanne, France
S. Beauceron, N. Beaupere, G. Boudoul, S. Brochet, C.A. Carrillo Montoya, J. Chasserat, R. Chierici, D. Contardo[2], P. Depasse, H. El Mamouni, J. Fan, J. Fay, S. Gascon, M. Gouzevitch, B. Ille, T. Kurca, M. Lethuillier, L. Mirabito, S. Perries, J.D. Ruiz Alvarez, L. Sgandurra, V. Sordini, M. Vander Donckt, P. Verdier, S. Viret, H. Xiao

Institute of High Energy Physics and Informatization, Tbilisi State University, Tbilisi, Georgia
Z. Tsamalaidze[16]

RWTH Aachen University, I. Physikalisches Institut, Aachen, Germany
C. Autermann, S. Beranek, M. Bontenackels, B. Calpas, M. Edelhoff, L. Feld, O. Hindrichs, K. Klein, A. Ostapchuk, A. Perieanu, F. Raupach, J. Sammet, S. Schael, D. Sprenger, H. Weber, B. Wittmer, V. Zhukov[5]

RWTH Aachen University, III. Physikalisches Institut A, Aachen, Germany
M. Ata, J. Caudron, E. Dietz-Laursonn, D. Duchardt, M. Erdmann, R. Fischer, A. Güth, T. Hebbeker, C. Heidemann, K. Hoepfner, D. Klingebiel, S. Knutzen, P. Kreuzer, M. Merschmeyer, A. Meyer, M. Olschewski, K. Padeken, P. Papacz, H. Reithler, S.A. Schmitz, L. Sonnenschein, D. Teyssier, S. Thüer, M. Weber

RWTH Aachen University, III. Physikalisches Institut B, Aachen, Germany
V. Cherepanov, Y. Erdogan, G. Flügge, H. Geenen, M. Geisler, W. Haj Ahmad, F. Hoehle, B. Kargoll, T. Kress, Y. Kuessel, J. Lingemann[2], A. Nowack, I.M. Nugent, L. Perchalla, O. Pooth, A. Stahl

Deutsches Elektronen-Synchrotron, Hamburg, Germany
I. Asin, N. Bartosik, J. Behr, W. Behrenhoff, U. Behrens, A.J. Bell, M. Bergholz[17], A. Bethani, K. Borras, A. Burgmeier, A. Cakir, L. Calligaris, A. Campbell, S. Choudhury, F. Costanza, C. Diez Pardos, S. Dooling, T. Dorland, G. Eckerlin, D. Eckstein, T. Eichhorn, G. Flucke, A. Geiser, A. Grebenyuk, P. Gunnellini, S. Habib, J. Hauk, G. Hellwig, M. Hempel, D. Horton, H. Jung, M. Kasemann, P. Katsas, J. Kieseler, C. Kleinwort, M. Krämer, D. Krücker, W. Lange, J. Leonard, K. Lipka, W. Lohmann[17], B. Lutz, R. Mankel, I. Marfin, I.-A. Melzer-Pellmann, A.B. Meyer, J. Mnich, A. Mussgiller, S. Naumann-Emme, O. Novgorodova, F. Nowak, E. Ntomari, H. Perrey, A. Petrukhin, D. Pitzl, R. Placakyte, A. Raspereza, P.M. Ribeiro Cipriano, C. Riedl, E. Ron, M.Ö. Sahin, J. Salfeld-Nebgen, P. Saxena, R. Schmidt[17], T. Schoerner-Sadenius, M. Schröder, M. Stein, A.D.R. Vargas Trevino, R. Walsh, C. Wissing

University of Hamburg, Hamburg, Germany
M. Aldaya Martin, V. Blobel, H. Enderle, J. Erfle, E. Garutti, K. Goebel, M. Görner, M. Gosselink, J. Haller, R.S. Höing, H. Kirschenmann, R. Klanner, R. Kogler, J. Lange, T. Lapsien, T. Lenz, I. Marchesini, J. Ott, T. Peiffer, N. Pietsch, D. Rathjens, C. Sander, H. Schettler, P. Schleper, E. Schlieckau, A. Schmidt, M. Seidel, J. Sibille[18], V. Sola, H. Stadie, G. Steinbrück, D. Troendle, E. Usai, L. Vanelderen

Institut für Experimentelle Kernphysik, Karlsruhe, Germany
C. Barth, C. Baus, J. Berger, C. Böser, E. Butz, T. Chwalek, W. De Boer, A. Descroix, A. Dierlamm, M. Feindt, M. Guthoff[2], F. Hartmann[2], T. Hauth[2], H. Held, K.H. Hoffmann, U. Husemann, I. Katkov[5], A. Kornmayer[2], E. Kuznetsova, P. Lobelle Pardo, D. Martschei, M.U. Mozer, Th. Müller, M. Niegel, A. Nürnberg, O. Oberst, G. Quast, K. Rabbertz, F. Ratnikov, S. Röcker, F.-P. Schilling, G. Schott, H.J. Simonis, F.M. Stober, R. Ulrich, J. Wagner-Kuhr, S. Wayand, T. Weiler, R. Wolf, M. Zeise

Institute of Nuclear and Particle Physics (INPP), NCSR Demokritos, Aghia Paraskevi, Greece
G. Anagnostou, G. Daskalakis, T. Geralis, S. Kesisoglou, A. Kyriakis, D. Loukas, A. Markou, C. Markou, A. Psallidas, I. Topsis-Giotis

University of Athens, Athens, Greece
L. Gouskos, A. Panagiotou, N. Saoulidou, E. Stiliaris

University of Ioánnina, Ioánnina, Greece
X. Aslanoglou, I. Evangelou[2], G. Flouris, C. Foudas[2], J. Jones, P. Kokkas, N. Manthos, I. Papadopoulos, E. Paradas

Wigner Research Centre for Physics, Budapest, Hungary
G. Bencze[2], C. Hajdu, P. Hidas, D. Horvath[19], F. Sikler, V. Veszpremi, G. Vesztergombi[20], A.J. Zsigmond

Institute of Nuclear Research ATOMKI, Debrecen, Hungary
N. Beni, S. Czellar, J. Molnar, J. Palinkas, Z. Szillasi

University of Debrecen, Debrecen, Hungary
J. Karancsi, P. Raics, Z.L. Trocsanyi, B. Ujvari

National Institute of Science Education and Research, Bhubaneswar, India
S.K. Swain

Panjab University, Chandigarh, India
S.B. Beri, V. Bhatnagar, N. Dhingra, R. Gupta, M. Kaur, M. Mittal, N. Nishu, A. Sharma, J.B. Singh

University of Delhi, Delhi, India
Ashok Kumar, Arun Kumar, S. Ahuja, A. Bhardwaj, B.C. Choudhary, A. Kumar, S. Malhotra, M. Naimuddin, K. Ranjan, V. Sharma, R.K. Shivpuri

Saha Institute of Nuclear Physics, Kolkata, India
S. Banerjee, S. Bhattacharya, K. Chatterjee, S. Dutta, B. Gomber, Sa. Jain, Sh. Jain, R. Khurana, A. Modak, S. Mukherjee, D. Roy, S. Sarkar, M. Sharan, A.P. Singh

Bhabha Atomic Research Centre, Mumbai, India
A. Abdulsalam, D. Dutta, S. Kailas, V. Kumar, A.K. Mohanty[2], L.M. Pant, P. Shukla, A. Topkar

Tata Institute of Fundamental Research - EHEP, Mumbai, India
T. Aziz, R.M. Chatterjee, S. Ganguly, S. Ghosh, M. Guchait[21], A. Gurtu[22], G. Kole, S. Kumar, M. Maity[23], G. Majumder, K. Mazumdar, G.B. Mohanty, B. Parida, K. Sudhakar, N. Wickramage[24]

Tata Institute of Fundamental Research - HECR, Mumbai, India
S. Banerjee, S. Dugad

Institute for Research in Fundamental Sciences (IPM), Tehran, Iran
H. Arfaei, H. Bakhshiansohi, H. Behnamian, S.M. Etesami[25], A. Fahim[26], A. Jafari, M. Khakzad, M. Mohammadi Najafabadi, M. Naseri, S. Paktinat Mehdiabadi, B. Safarzadeh[27], M. Zeinali

University College Dublin, Dublin, Ireland
M. Grunewald

INFN Sezione di Bari [a], Università di Bari [b], Politecnico di Bari [c], Bari, Italy
M. Abbrescia[a,b], L. Barbone[a,b], C. Calabria[a,b], S.S. Chhibra[a,b], A. Colaleo[a], D. Creanza[a,c], N. De Filippis[a,c], M. De Palma[a,b], L. Fiore[a], G. Iaselli[a,c], G. Maggi[a,c], M. Maggi[a], B. Marangelli[a,b], S. My[a,c], S. Nuzzo[a,b], N. Pacifico[a], A. Pompili[a,b], G. Pugliese[a,c], R. Radogna[a,b], G. Selvaggi[a,b], L. Silvestris[a], G. Singh[a,b], R. Venditti[a,b], P. Verwilligen[a], G. Zito[a]

INFN Sezione di Bologna [a], Università di Bologna [b], Bologna, Italy
G. Abbiendi[a], A.C. Benvenuti[a], D. Bonacorsi[a,b], S. Braibant-Giacomelli[a,b], L. Brigliadori[a,b], R. Campanini[a,b], P. Capiluppi[a,b], A. Castro[a,b], F.R. Cavallo[a], G. Codispoti[a,b], M. Cuffiani[a,b], G.M. Dallavalle[a], F. Fabbri[a], A. Fanfani[a,b], D. Fasanella[a,b], P. Giacomelli[a], C. Grandi[a], L. Guiducci[a,b], S. Marcellini[a], G. Masetti[a], M. Meneghelli[a,b], A. Montanari[a], F.L. Navarria[a,b], F. Odorici[a], A. Perrotta[a], F. Primavera[a,b], A.M. Rossi[a,b], T. Rovelli[a,b], G.P. Siroli[a,b], N. Tosi[a,b], R. Travaglini[a,b]

INFN Sezione di Catania [a], Università di Catania [b], CSFNSM [c], Catania, Italy
S. Albergo[a,b], G. Cappello[a], M. Chiorboli[a,b], S. Costa[a,b], F. Giordano[a,c,2], R. Potenza[a,b], A. Tricomi[a,b], C. Tuve[a,b]

INFN Sezione di Firenze [a], Università di Firenze [b], Firenze, Italy
G. Barbagli[a], V. Ciulli[a,b], C. Civinini[a], R. D'Alessandro[a,b], E. Focardi[a,b], E. Gallo[a], S. Gonzi[a,b], V. Gori[a,b], P. Lenzi[a,b], M. Meschini[a], S. Paoletti[a], G. Sguazzoni[a], A. Tropiano[a,b]

INFN Laboratori Nazionali di Frascati, Frascati, Italy
L. Benussi, S. Bianco, F. Fabbri, D. Piccolo

INFN Sezione di Genova [a], Università di Genova [b], Genova, Italy
P. Fabbricatore[a], R. Ferretti[a,b], F. Ferro[a], M. Lo Vetere[a,b], R. Musenich[a], E. Robutti[a], S. Tosi[a,b]

INFN Sezione di Milano-Bicocca [a], Università di Milano-Bicocca [b], Milano, Italy
M.E. Dinardo[a,b], S. Fiorendi[a,b,2], S. Gennai[a], R. Gerosa, A. Ghezzi[a,b], P. Govoni[a,b], M.T. Lucchini[a,b,2], S. Malvezzi[a], R.A. Manzoni[a,b,2], A. Martelli[a,b,2], B. Marzocchi, D. Menasce[a], L. Moroni[a], M. Paganoni[a,b], D. Pedrini[a], S. Ragazzi[a,b], N. Redaelli[a], T. Tabarelli de Fatis[a,b]

INFN Sezione di Napoli [a], Università di Napoli 'Federico II' [b], Università della Basilicata (Potenza) [c], Università G. Marconi (Roma) [d], Napoli, Italy
S. Buontempo[a], N. Cavallo[a,c], S. Di Guida[a,d], F. Fabozzi[a,c], A.O.M. Iorio[a,b], L. Lista[a], S. Meola[a,d,2], M. Merola[a], P. Paolucci[a,2]

INFN Sezione di Padova [a], Università di Padova [b], Università di Trento (Trento) [c], Padova, Italy
P. Azzi[a], N. Bacchetta[a], D. Bisello[a,b], A. Branca[a,b], R. Carlin[a,b], P. Checchia[a], T. Dorigo[a], M. Galanti[a,b,2], F. Gasparini[a,b], U. Gasparini[a,b], P. Giubilato[a,b], A. Gozzelino[a], K. Kanishchev[a,c], S. Lacaprara[a], I. Lazzizzera[a,c], M. Margoni[a,b], A.T. Meneguzzo[a,b], F. Montecassiano[a], M. Passaseo[a], J. Pazzini[a,b], N. Pozzobon[a,b], P. Ronchese[a,b], F. Simonetto[a,b], E. Torassa[a], M. Tosi[a,b], S. Vanini[a,b], P. Zotto[a,b], A. Zucchetta[a,b], G. Zumerle[a,b]

INFN Sezione di Pavia [a], Università di Pavia [b], Pavia, Italy
M. Gabusi[a,b], S.P. Ratti[a,b], C. Riccardi[a,b], P. Salvini[a], P. Vitulo[a,b]

INFN Sezione di Perugia [a], Università di Perugia [b], Perugia, Italy
M. Biasini[a,b], G.M. Bilei[a], L. Fanò[a,b], P. Lariccia[a,b], G. Mantovani[a,b], M. Menichelli[a], F. Romeo[a,b], A. Saha[a], A. Santocchia[a,b], A. Spiezia[a,b]

INFN Sezione di Pisa [a], Università di Pisa [b], Scuola Normale Superiore di Pisa [c], Pisa, Italy
K. Androsov[a,28], P. Azzurri[a], G. Bagliesi[a], J. Bernardini[a], T. Boccali[a], G. Broccolo[a,c], R. Castaldi[a], M.A. Ciocci[a,28], R. Dell'Orso[a], S. Donato[a,c], F. Fiori[a,c], L. Foà[a,c], A. Giassi[a], M.T. Grippo[a,28], A. Kraan[a], F. Ligabue[a,c], T. Lomtadze[a], L. Martini[a,b], A. Messineo[a,b], C.S. Moon[a,29], F. Palla[a,2], A. Rizzi[a,b], A. Savoy-Navarro[a,30], A.T. Serban[a], P. Spagnolo[a], P. Squillacioti[a,28], R. Tenchini[a], G. Tonelli[a,b], A. Venturi[a], P.G. Verdini[a], C. Vernieri[a,c]

INFN Sezione di Roma [a], Università di Roma [b], Roma, Italy
L. Barone[a,b], F. Cavallari[a], D. Del Re[a,b], M. Diemoz[a], M. Grassi[a,b], C. Jorda[a], E. Longo[a,b], F. Margaroli[a,b], P. Meridiani[a], F. Micheli[a,b], S. Nourbakhsh[a,b], G. Organtini[a,b], R. Paramatti[a], S. Rahatlou[a,b], C. Rovelli[a], L. Soffi[a,b], P. Traczyk[a,b]

INFN Sezione di Torino [a], Università di Torino [b], Università del Piemonte Orientale (Novara) [c], Torino, Italy
N. Amapane[a,b], R. Arcidiacono[a,c], S. Argiro[a,b], M. Arneodo[a,c], R. Bellan[a,b], C. Biino[a], N. Cartiglia[a], S. Casasso[a,b], M. Costa[a,b], A. Degano[a,b], N. Demaria[a], C. Mariotti[a], S. Maselli[a], E. Migliore[a,b], V. Monaco[a,b], M. Musich[a], M.M. Obertino[a,c], G. Ortona[a,b], L. Pacher[a,b], N. Pastrone[a], M. Pelliccioni[a,2], A. Potenza[a,b], A. Romero[a,b], M. Ruspa[a,c], R. Sacchi[a,b], A. Solano[a,b], A. Staiano[a], U. Tamponi[a]

INFN Sezione di Trieste [a], Università di Trieste [b], Trieste, Italy
S. Belforte[a], V. Candelise[a,b], M. Casarsa[a], F. Cossutti[a], G. Della Ricca[a,b], B. Gobbo[a], C. La Licata[a,b], M. Marone[a,b], D. Montanino[a,b], A. Penzo[a], A. Schizzi[a,b], T. Umer[a,b], A. Zanetti[a]

Kangwon National University, Chunchon, Korea
S. Chang, T.Y. Kim, S.K. Nam

Kyungpook National University, Daegu, Korea
D.H. Kim, G.N. Kim, J.E. Kim, M.S. Kim, D.J. Kong, S. Lee, Y.D. Oh, H. Park, A. Sakharov, D.C. Son

Chonnam National University, Institute for Universe and Elementary Particles, Kwangju, Korea
J.Y. Kim, Zero J. Kim, S. Song

Korea University, Seoul, Korea
S. Choi, D. Gyun, B. Hong, M. Jo, H. Kim, Y. Kim, B. Lee, K.S. Lee, S.K. Park, Y. Roh

University of Seoul, Seoul, Korea
M. Choi, J.H. Kim, C. Park, I.C. Park, S. Park, G. Ryu

Sungkyunkwan University, Suwon, Korea
Y. Choi, Y.K. Choi, J. Goh, E. Kwon, J. Lee, H. Seo, I. Yu

Vilnius University, Vilnius, Lithuania
A. Juodagalvis

National Centre for Particle Physics, Universiti Malaya, Kuala Lumpur, Malaysia
J.R. Komaragiri

Centro de Investigacion y de Estudios Avanzados del IPN, Mexico City, Mexico
H. Castilla-Valdez, E. De La Cruz-Burelo, I. Heredia-de La Cruz[31], R. Lopez-Fernandez, J. Martínez-Ortega, A. Sanchez-Hernandez, L.M. Villasenor-Cendejas

Universidad Iberoamericana, Mexico City, Mexico
S. Carrillo Moreno, F. Vazquez Valencia

Benemerita Universidad Autonoma de Puebla, Puebla, Mexico
H.A. Salazar Ibarguen

Universidad Autónoma de San Luis Potosí, San Luis Potosí, Mexico
E. Casimiro Linares, A. Morelos Pineda

University of Auckland, Auckland, New Zealand
D. Krofcheck

University of Canterbury, Christchurch, New Zealand
P.H. Butler, R. Doesburg, S. Reucroft

National Centre for Physics, Quaid-I-Azam University, Islamabad, Pakistan
A. Ahmad, M. Ahmad, M.I. Asghar, J. Butt, Q. Hassan, H.R. Hoorani, W.A. Khan, T. Khurshid, S. Qazi, M.A. Shah, M. Shoaib

National Centre for Nuclear Research, Swierk, Poland
H. Bialkowska, M. Bluj[32], B. Boimska, T. Frueboes, M. Górski, M. Kazana, K. Nawrocki, K. Romanowska-Rybinska, M. Szleper, G. Wrochna, P. Zalewski

Institute of Experimental Physics, Faculty of Physics, University of Warsaw, Warsaw, Poland
G. Brona, K. Bunkowski, M. Cwiok, W. Dominik, K. Doroba, A. Kalinowski, M. Konecki, J. Krolikowski, M. Misiura, W. Wolszczak

Laboratório de Instrumentação e Física Experimental de Partículas, Lisboa, Portugal
P. Bargassa, C. Beirão Da Cruz E Silva, P. Faccioli, P.G. Ferreira Parracho, M. Gallinaro, F. Nguyen, J. Rodrigues Antunes, J. Seixas, J. Varela, P. Vischia

Joint Institute for Nuclear Research, Dubna, Russia
I. Golutvin, A. Kamenev, V. Karjavin, V. Konoplyanikov, V. Korenkov, A. Lanev, A. Malakhov, V. Matveev[33], P. Moisenz, V. Palichik, V. Perelygin, M. Savina, S. Shmatov, S. Shulha, N. Skatchkov, V. Smirnov, E. Tikhonenko, A. Zarubin

Petersburg Nuclear Physics Institute, Gatchina (St. Petersburg), Russia
V. Golovtsov, Y. Ivanov, V. Kim[34], P. Levchenko, V. Murzin, V. Oreshkin, I. Smirnov, V. Sulimov, L. Uvarov, S. Vavilov, A. Vorobyev, An. Vorobyev

Institute for Nuclear Research, Moscow, Russia
Yu. Andreev, A. Dermenev, S. Gninenko, N. Golubev, M. Kirsanov, N. Krasnikov, A. Pashenkov, D. Tlisov, A. Toropin

Institute for Theoretical and Experimental Physics, Moscow, Russia
V. Epshteyn, V. Gavrilov, N. Lychkovskaya, V. Popov, G. Safronov, S. Semenov, A. Spiridonov, V. Stolin, E. Vlasov, A. Zhokin

P.N. Lebedev Physical Institute, Moscow, Russia
V. Andreev, M. Azarkin, I. Dremin, M. Kirakosyan, A. Leonidov, G. Mesyats, S.V. Rusakov, A. Vinogradov

Skobeltsyn Institute of Nuclear Physics, Lomonosov Moscow State University, Moscow, Russia
A. Belyaev, E. Boos, M. Dubinin[7], L. Dudko, A. Ershov, A. Gribushin, V. Klyukhin, O. Kodolova, I. Lokhtin, S. Obraztsov, S. Petrushanko, V. Savrin, A. Snigirev

State Research Center of Russian Federation, Institute for High Energy Physics, Protvino, Russia
I. Azhgirey, I. Bayshev, S. Bitioukov, V. Kachanov, A. Kalinin, D. Konstantinov, V. Krychkine, V. Petrov, R. Ryutin, A. Sobol, L. Tourtchanovitch, S. Troshin, N. Tyurin, A. Uzunian, A. Volkov

University of Belgrade, Faculty of Physics and Vinca Institute of Nuclear Sciences, Belgrade, Serbia
P. Adzic[35], M. Dordevic, M. Ekmedzic, J. Milosevic

Centro de Investigaciones Energéticas Medioambientales y Tecnológicas (CIEMAT), Madrid, Spain
M. Aguilar-Benitez, J. Alcaraz Maestre, C. Battilana, E. Calvo, M. Cerrada, M. Chamizo Llatas[2], N. Colino, B. De La Cruz, A. Delgado Peris, D. Domínguez Vázquez, C. Fernandez Bedoya, J.P. Fernández Ramos, A. Ferrando, J. Flix, M.C. Fouz, P. Garcia-Abia, O. Gonzalez Lopez, S. Goy Lopez, J.M. Hernandez, M.I. Josa, G. Merino, E. Navarro De Martino, A. Pérez-Calero Yzquierdo, J. Puerta Pelayo, A. Quintario Olmeda, I. Redondo, L. Romero, M.S. Soares, C. Willmott

Universidad Autónoma de Madrid, Madrid, Spain
C. Albajar, J.F. de Trocóniz, M. Missiroli

Universidad de Oviedo, Oviedo, Spain
H. Brun, J. Cuevas, J. Fernandez Menendez, S. Folgueras, I. Gonzalez Caballero, L. Lloret Iglesias

Instituto de Física de Cantabria (IFCA), CSIC-Universidad de Cantabria, Santander, Spain
J.A. Brochero Cifuentes, I.J. Cabrillo, A. Calderon, J. Duarte Campderros, M. Fernandez, G. Gomez, J. Gonzalez Sanchez, A. Graziano, A. Lopez Virto, J. Marco, R. Marco, C. Martinez Rivero, F. Matorras, F.J. Munoz Sanchez, J. Piedra Gomez, T. Rodrigo, A.Y. Rodríguez-Marrero, A. Ruiz-Jimeno, L. Scodellaro, I. Vila, R. Vilar Cortabitarte

CERN, European Organization for Nuclear Research, Geneva, Switzerland
D. Abbaneo, E. Auffray, G. Auzinger, M. Bachtis, P. Baillon, A.H. Ball, D. Barney, A. Benaglia, J. Bendavid, L. Benhabib, J.F. Benitez, C. Bernet[8], G. Bianchi, P. Bloch, A. Bocci, A. Bonato, O. Bondu, C. Botta, H. Breuker, T. Camporesi, G. Cerminara, T. Christiansen, J.A. Coarasa Perez, S. Colafranceschi[36], M. D'Alfonso, D. d'Enterria, A. Dabrowski, A. David, F. De Guio, A. De Roeck, S. De Visscher, M. Dobson, N. Dupont-Sagorin, A. Elliott-Peisert, J. Eugster, G. Franzoni, W. Funk, M. Giffels, D. Gigi, K. Gill, D. Giordano, M. Girone, M. Giunta, F. Glege, R. Gomez-Reino Garrido, S. Gowdy, R. Guida, J. Hammer, M. Hansen, P. Harris, J. Hegeman, V. Innocente, P. Janot, E. Karavakis, K. Kousouris, K. Krajczar, P. Lecoq, C. Lourenço, N. Magini, L. Malgeri, M. Mannelli, L. Masetti, F. Meijers, S. Mersi, E. Meschi, F. Moortgat,

M. Mulders, P. Musella, L. Orsini, E. Palencia Cortezon, L. Pape, E. Perez, L. Perrozzi, A. Petrilli, G. Petrucciani, A. Pfeiffer, M. Pierini, M. Pimiä, D. Piparo, M. Plagge, A. Racz, W. Reece, G. Rolandi[37], M. Rovere, H. Sakulin, F. Santanastasio, C. Schäfer, C. Schwick, S. Sekmen, A. Sharma, P. Siegrist, P. Silva, M. Simon, P. Sphicas[38], D. Spiga, J. Steggemann, B. Stieger, M. Stoye, D. Treille, A. Tsirou, G.I. Veres[20], J.R. Vlimant, H.K. Wöhri, W.D. Zeuner

Paul Scherrer Institut, Villigen, Switzerland
W. Bertl, K. Deiters, W. Erdmann, R. Horisberger, Q. Ingram, H.C. Kaestli, S. König, D. Kotlinski, U. Langenegger, D. Renker, T. Rohe

Institute for Particle Physics, ETH Zurich, Zurich, Switzerland
F. Bachmair, L. Bäni, L. Bianchini, P. Bortignon, M.A. Buchmann, B. Casal, N. Chanon, A. Deisher, G. Dissertori, M. Dittmar, M. Donegà, M. Dünser, P. Eller, C. Grab, D. Hits, W. Lustermann, B. Mangano, A.C. Marini, P. Martinez Ruiz del Arbol, D. Meister, N. Mohr, C. Nägeli[39], P. Nef, F. Nessi-Tedaldi, F. Pandolfi, F. Pauss, M. Peruzzi, M. Quittnat, L. Rebane, F.J. Ronga, M. Rossini, A. Starodumov[40], M. Takahashi, K. Theofilatos, R. Wallny, H.A. Weber

Universität Zürich, Zurich, Switzerland
C. Amsler[41], M.F. Canelli, V. Chiochia, A. De Cosa, C. Favaro, A. Hinzmann, T. Hreus, M. Ivova Rikova, B. Kilminster, B. Millan Mejias, J. Ngadiuba, P. Robmann, H. Snoek, S. Taroni, M. Verzetti, Y. Yang

National Central University, Chung-Li, Taiwan
M. Cardaci, K.H. Chen, C. Ferro, C.M. Kuo, S.W. Li, W. Lin, Y.J. Lu, R. Volpe, S.S. Yu

National Taiwan University (NTU), Taipei, Taiwan
P. Bartalini, P. Chang, Y.H. Chang, Y.W. Chang, Y. Chao, K.F. Chen, P.H. Chen, C. Dietz, U. Grundler, W.-S. Hou, Y. Hsiung, K.Y. Kao, Y.J. Lei, Y.F. Liu, R.-S. Lu, D. Majumder, E. Petrakou, X. Shi, J.G. Shiu, Y.M. Tzeng, M. Wang, R. Wilken

Chulalongkorn University, Bangkok, Thailand
B. Asavapibhop, N. Suwonjandee

Cukurova University, Adana, Turkey
A. Adiguzel, M.N. Bakirci[42], S. Cerci[43], C. Dozen, I. Dumanoglu, E. Eskut, S. Girgis, G. Gokbulut, E. Gurpinar, I. Hos, E.E. Kangal, A. Kayis Topaksu, G. Onengut[44], K. Ozdemir, S. Ozturk[42], A. Polatoz, K. Sogut[45], D. Sunar Cerci[43], B. Tali[43], H. Topakli[42], M. Vergili

Middle East Technical University, Physics Department, Ankara, Turkey
I.V. Akin, T. Aliev, B. Bilin, S. Bilmis, M. Deniz, H. Gamsizkan, A.M. Guler, G. Karapinar[46], K. Ocalan, A. Ozpineci, M. Serin, R. Sever, U.E. Surat, M. Yalvac, M. Zeyrek

Bogazici University, Istanbul, Turkey
E. Gülmez, B. Isildak[47], M. Kaya[48], O. Kaya[48], S. Ozkorucuklu[49]

Istanbul Technical University, Istanbul, Turkey
H. Bahtiyar[50], E. Barlas, K. Cankocak, Y.O. Günaydin[51], F.I. Vardarlı, M. Yücel

National Scientific Center, Kharkov Institute of Physics and Technology, Kharkov, Ukraine
L. Levchuk, P. Sorokin

University of Bristol, Bristol, United Kingdom
J.J. Brooke, E. Clement, D. Cussans, H. Flacher, R. Frazier, J. Goldstein, M. Grimes, G.P. Heath, H.F. Heath, J. Jacob, L. Kreczko, C. Lucas, Z. Meng, D.M. Newbold[52], S. Paramesvaran, A. Poll, S. Senkin, V.J. Smith, T. Williams

Rutherford Appleton Laboratory, Didcot, United Kingdom
K.W. Bell, A. Belyaev[53], C. Brew, R.M. Brown, D.J.A. Cockerill, J.A. Coughlan, K. Harder, S. Harper, J. Ilic, E. Olaiya, D. Petyt, C.H. Shepherd-Themistocleous, A. Thea, I.R. Tomalin, W.J. Womersley, S.D. Worm

Imperial College, London, United Kingdom
M. Baber, R. Bainbridge, O. Buchmuller, D. Burton, D. Colling, N. Cripps, M. Cutajar, P. Dauncey, G. Davies, M. Della Negra, W. Ferguson, J. Fulcher, D. Futyan, A. Gilbert, A. Guneratne Bryer, G. Hall, Z. Hatherell, J. Hays, G. Iles, M. Jarvis, G. Karapostoli, M. Kenzie, R. Lane, R. Lucas[52], L. Lyons, A.-M. Magnan, J. Marrouche, B. Mathias, R. Nandi, J. Nash, A. Nikitenko[40], J. Pela, M. Pesaresi, K. Petridis, M. Pioppi[54], D.M. Raymond, S. Rogerson, A. Rose, C. Seez, P. Sharp†, A. Sparrow, A. Tapper, M. Vazquez Acosta, T. Virdee, S. Wakefield, N. Wardle

Brunel University, Uxbridge, United Kingdom
J.E. Cole, P.R. Hobson, A. Khan, P. Kyberd, D. Leggat, D. Leslie, W. Martin, I.D. Reid, P. Symonds, L. Teodorescu, M. Turner

Baylor University, Waco, USA
J. Dittmann, K. Hatakeyama, A. Kasmi, H. Liu, T. Scarborough

The University of Alabama, Tuscaloosa, USA
O. Charaf, S.I. Cooper, C. Henderson, P. Rumerio

Boston University, Boston, USA
A. Avetisyan, T. Bose, C. Fantasia, A. Heister, P. Lawson, D. Lazic, C. Richardson, J. Rohlf, D. Sperka, J. St. John, L. Sulak

Brown University, Providence, USA
J. Alimena, S. Bhattacharya, G. Christopher, D. Cutts, Z. Demiragli, A. Ferapontov, A. Garabedian, U. Heintz, S. Jabeen, G. Kukartsev, E. Laird, G. Landsberg, M. Luk, M. Narain, M. Segala, T. Sinthuprasith, T. Speer, J. Swanson

University of California, Davis, Davis, USA
R. Breedon, G. Breto, M. Calderon De La Barca Sanchez, S. Chauhan, M. Chertok, J. Conway, R. Conway, P.T. Cox, R. Erbacher, M. Gardner, W. Ko, A. Kopecky, R. Lander, T. Miceli, M. Mulhearn, D. Pellett, J. Pilot, F. Ricci-Tam, B. Rutherford, M. Searle, S. Shalhout, J. Smith, M. Squires, M. Tripathi, S. Wilbur, R. Yohay

University of California, Los Angeles, USA
V. Andreev, D. Cline, R. Cousins, S. Erhan, P. Everaerts, C. Farrell, M. Felcini, J. Hauser, M. Ignatenko, C. Jarvis, G. Rakness, P. Schlein†, E. Takasugi, V. Valuev, M. Weber

University of California, Riverside, Riverside, USA
J. Babb, R. Clare, J. Ellison, J.W. Gary, G. Hanson, J. Heilman, P. Jandir, F. Lacroix, H. Liu, O.R. Long, A. Luthra, M. Malberti, H. Nguyen, A. Shrinivas, J. Sturdy, S. Sumowidagdo, S. Wimpenny

University of California, San Diego, La Jolla, USA
W. Andrews, J.G. Branson, G.B. Cerati, S. Cittolin, R.T. D'Agnolo, D. Evans, A. Holzner, R. Kelley, D. Kovalskyi, M. Lebourgeois, J. Letts, I. Macneill, S. Padhi, C. Palmer, M. Pieri, M. Sani, V. Sharma, S. Simon, E. Sudano, M. Tadel, Y. Tu, A. Vartak, S. Wasserbaech[55], F. Würthwein, A. Yagil, J. Yoo

University of California, Santa Barbara, Santa Barbara, USA
D. Barge, J. Bradmiller-Feld, C. Campagnari, T. Danielson, A. Dishaw, K. Flowers, M. Franco Sevilla, P. Geffert, C. George, F. Golf, J. Incandela, C. Justus, R. Magaña Villalba, N. Mccoll, V. Pavlunin, J. Richman, R. Rossin, D. Stuart, W. To, C. West

California Institute of Technology, Pasadena, USA
A. Apresyan, A. Bornheim, J. Bunn, Y. Chen, E. Di Marco, J. Duarte, D. Kcira, A. Mott, H.B. Newman, C. Pena, C. Rogan, M. Spiropulu, V. Timciuc, R. Wilkinson, S. Xie, R.Y. Zhu

Carnegie Mellon University, Pittsburgh, USA
V. Azzolini, A. Calamba, R. Carroll, T. Ferguson, Y. Iiyama, D.W. Jang, M. Paulini, J. Russ, H. Vogel, I. Vorobiev

University of Colorado at Boulder, Boulder, USA
J.P. Cumalat, B.R. Drell, W.T. Ford, A. Gaz, E. Luiggi Lopez, U. Nauenberg, J.G. Smith, K. Stenson, K.A. Ulmer, S.R. Wagner

Cornell University, Ithaca, USA
J. Alexander, A. Chatterjee, J. Chu, N. Eggert, L.K. Gibbons, W. Hopkins, A. Khukhunaishvili, B. Kreis, N. Mirman, G. Nicolas Kaufman, J.R. Patterson, A. Ryd, E. Salvati, W. Sun, W.D. Teo, J. Thom, J. Thompson, J. Tucker, Y. Weng, L. Winstrom, P. Wittich

Fairfield University, Fairfield, USA
D. Winn

Fermi National Accelerator Laboratory, Batavia, USA
S. Abdullin, M. Albrow, J. Anderson, G. Apollinari, L.A.T. Bauerdick, A. Beretvas, J. Berryhill, P.C. Bhat, K. Burkett, J.N. Butler, V. Chetluru, H.W.K. Cheung, F. Chlebana, S. Cihangir, V.D. Elvira, I. Fisk, J. Freeman, Y. Gao, E. Gottschalk, L. Gray, D. Green, S. Grünendahl, O. Gutsche, D. Hare, R.M. Harris, J. Hirschauer, B. Hooberman, S. Jindariani, M. Johnson, U. Joshi, K. Kaadze, B. Klima, S. Kwan, J. Linacre, D. Lincoln, R. Lipton, T. Liu, J. Lykken, K. Maeshima, J.M. Marraffino, V.I. Martinez Outschoorn, S. Maruyama, D. Mason, P. McBride, K. Mishra, S. Mrenna, Y. Musienko[33], S. Nahn, C. Newman-Holmes, V. O'Dell, O. Prokofyev, N. Ratnikova, E. Sexton-Kennedy, S. Sharma, A. Soha, W.J. Spalding, L. Spiegel, L. Taylor, S. Tkaczyk, N.V. Tran, L. Uplegger, E.W. Vaandering, R. Vidal, A. Whitbeck, J. Whitmore, W. Wu, F. Yang, J.C. Yun

University of Florida, Gainesville, USA
D. Acosta, P. Avery, D. Bourilkov, T. Cheng, S. Das, M. De Gruttola, G.P. Di Giovanni, D. Dobur, R.D. Field, M. Fisher, Y. Fu, I.K. Furic, J. Hugon, B. Kim, J. Konigsberg, A. Korytov, A. Kropivnitskaya, T. Kypreos, J.F. Low, K. Matchev, P. Milenovic[56], G. Mitselmakher, L. Muniz, A. Rinkevicius, L. Shchutska, N. Skhirtladze, M. Snowball, J. Yelton, M. Zakaria

Florida International University, Miami, USA
V. Gaultney, S. Hewamanage, S. Linn, P. Markowitz, G. Martinez, J.L. Rodriguez

Florida State University, Tallahassee, USA
T. Adams, A. Askew, J. Bochenek, J. Chen, B. Diamond, J. Haas, S. Hagopian, V. Hagopian, K.F. Johnson, H. Prosper, V. Veeraraghavan, M. Weinberg

Florida Institute of Technology, Melbourne, USA
M.M. Baarmand, B. Dorney, M. Hohlmann, H. Kalakhety, F. Yumiceva

University of Illinois at Chicago (UIC), Chicago, USA
M.R. Adams, L. Apanasevich, V.E. Bazterra, R.R. Betts, I. Bucinskaite, R. Cavanaugh,

O. Evdokimov, L. Gauthier, C.E. Gerber, D.J. Hofman, S. Khalatyan, P. Kurt, D.H. Moon, C. O'Brien, C. Silkworth, P. Turner, N. Varelas

The University of Iowa, Iowa City, USA
U. Akgun, E.A. Albayrak[50], B. Bilki[57], W. Clarida, K. Dilsiz, F. Duru, M. Haytmyradov, J.-P. Merlo, H. Mermerkaya[58], A. Mestvirishvili, A. Moeller, J. Nachtman, H. Ogul, Y. Onel, F. Ozok[50], R. Rahmat, S. Sen, P. Tan, E. Tiras, J. Wetzel, T. Yetkin[59], K. Yi

Johns Hopkins University, Baltimore, USA
B.A. Barnett, B. Blumenfeld, S. Bolognesi, D. Fehling, A.V. Gritsan, P. Maksimovic, C. Martin, M. Swartz

The University of Kansas, Lawrence, USA
P. Baringer, A. Bean, G. Benelli, J. Gray, R.P. Kenny III, M. Murray, D. Noonan, S. Sanders, J. Sekaric, R. Stringer, Q. Wang, J.S. Wood

Kansas State University, Manhattan, USA
A.F. Barfuss, I. Chakaberia, A. Ivanov, S. Khalil, M. Makouski, Y. Maravin, L.K. Saini, S. Shrestha, I. Svintradze

Lawrence Livermore National Laboratory, Livermore, USA
J. Gronberg, D. Lange, F. Rebassoo, D. Wright

University of Maryland, College Park, USA
A. Baden, B. Calvert, S.C. Eno, J.A. Gomez, N.J. Hadley, R.G. Kellogg, T. Kolberg, Y. Lu, M. Marionneau, A.C. Mignerey, K. Pedro, A. Skuja, J. Temple, M.B. Tonjes, S.C. Tonwar

Massachusetts Institute of Technology, Cambridge, USA
A. Apyan, R. Barbieri, G. Bauer, W. Busza, I.A. Cali, M. Chan, L. Di Matteo, V. Dutta, G. Gomez Ceballos, M. Goncharov, D. Gulhan, M. Klute, Y.S. Lai, Y.-J. Lee, A. Levin, P.D. Luckey, T. Ma, C. Paus, D. Ralph, C. Roland, G. Roland, G.S.F. Stephans, F. Stöckli, K. Sumorok, D. Velicanu, J. Veverka, B. Wyslouch, M. Yang, A.S. Yoon, M. Zanetti, V. Zhukova

University of Minnesota, Minneapolis, USA
B. Dahmes, A. De Benedetti, A. Gude, S.C. Kao, K. Klapoetke, Y. Kubota, J. Mans, N. Pastika, R. Rusack, A. Singovsky, N. Tambe, J. Turkewitz

University of Mississippi, Oxford, USA
J.G. Acosta, L.M. Cremaldi, R. Kroeger, S. Oliveros, L. Perera, D.A. Sanders, D. Summers

University of Nebraska-Lincoln, Lincoln, USA
E. Avdeeva, K. Bloom, S. Bose, D.R. Claes, A. Dominguez, R. Gonzalez Suarez, J. Keller, D. Knowlton, I. Kravchenko, J. Lazo-Flores, S. Malik, F. Meier, G.R. Snow

State University of New York at Buffalo, Buffalo, USA
J. Dolen, A. Godshalk, I. Iashvili, S. Jain, A. Kharchilava, A. Kumar, S. Rappoccio

Northeastern University, Boston, USA
G. Alverson, E. Barberis, D. Baumgartel, M. Chasco, J. Haley, A. Massironi, D. Nash, T. Orimoto, D. Trocino, D. Wood, J. Zhang

Northwestern University, Evanston, USA
A. Anastassov, K.A. Hahn, A. Kubik, L. Lusito, N. Mucia, N. Odell, B. Pollack, A. Pozdnyakov, M. Schmitt, S. Stoynev, K. Sung, M. Velasco, S. Won

University of Notre Dame, Notre Dame, USA
D. Berry, A. Brinkerhoff, K.M. Chan, A. Drozdetskiy, M. Hildreth, C. Jessop, D.J. Karmgard, N. Kellams, J. Kolb, K. Lannon, W. Luo, S. Lynch, N. Marinelli, D.M. Morse, T. Pearson, M. Planer, R. Ruchti, J. Slaunwhite, N. Valls, M. Wayne, M. Wolf, A. Woodard

The Ohio State University, Columbus, USA
L. Antonelli, B. Bylsma, L.S. Durkin, S. Flowers, C. Hill, R. Hughes, K. Kotov, T.Y. Ling, D. Puigh, M. Rodenburg, G. Smith, C. Vuosalo, B.L. Winer, H. Wolfe, H.W. Wulsin

Princeton University, Princeton, USA
E. Berry, P. Elmer, V. Halyo, P. Hebda, A. Hunt, P. Jindal, S.A. Koay, P. Lujan, D. Marlow, T. Medvedeva, M. Mooney, J. Olsen, P. Piroué, X. Quan, A. Raval, H. Saka, D. Stickland, C. Tully, J.S. Werner, S.C. Zenz, A. Zuranski

University of Puerto Rico, Mayaguez, USA
E. Brownson, A. Lopez, H. Mendez, J.E. Ramirez Vargas

Purdue University, West Lafayette, USA
E. Alagoz, D. Benedetti, G. Bolla, D. Bortoletto, M. De Mattia, A. Everett, Z. Hu, M.K. Jha, M. Jones, K. Jung, M. Kress, N. Leonardo, D. Lopes Pegna, V. Maroussov, P. Merkel, D.H. Miller, N. Neumeister, B.C. Radburn-Smith, I. Shipsey, D. Silvers, A. Svyatkovskiy, F. Wang, W. Xie, L. Xu, H.D. Yoo, J. Zablocki, Y. Zheng

Purdue University Calumet, Hammond, USA
N. Parashar

Rice University, Houston, USA
A. Adair, B. Akgun, K.M. Ecklund, F.J.M. Geurts, W. Li, B. Michlin, B.P. Padley, R. Redjimi, J. Roberts, J. Zabel

University of Rochester, Rochester, USA
B. Betchart, A. Bodek, R. Covarelli, P. de Barbaro, R. Demina, Y. Eshaq, T. Ferbel, A. Garcia-Bellido, P. Goldenzweig, J. Han, A. Harel, D.C. Miner, G. Petrillo, D. Vishnevskiy, M. Zielinski

The Rockefeller University, New York, USA
A. Bhatti, R. Ciesielski, L. Demortier, K. Goulianos, G. Lungu, S. Malik, C. Mesropian

Rutgers, The State University of New Jersey, Piscataway, USA
S. Arora, A. Barker, J.P. Chou, C. Contreras-Campana, E. Contreras-Campana, D. Duggan, J. Evans, D. Ferencek, Y. Gershtein, R. Gray, E. Halkiadakis, D. Hidas, A. Lath, S. Panwalkar, M. Park, R. Patel, V. Rekovic, J. Robles, S. Salur, S. Schnetzer, C. Seitz, S. Somalwar, R. Stone, S. Thomas, P. Thomassen, M. Walker

University of Tennessee, Knoxville, USA
K. Rose, S. Spanier, Z.C. Yang, A. York

Texas A&M University, College Station, USA
O. Bouhali[60], R. Eusebi, W. Flanagan, J. Gilmore, T. Kamon[61], V. Khotilovich, V. Krutelyov, R. Montalvo, I. Osipenkov, Y. Pakhotin, A. Perloff, J. Roe, A. Safonov, T. Sakuma, I. Suarez, A. Tatarinov, D. Toback

Texas Tech University, Lubbock, USA
N. Akchurin, C. Cowden, J. Damgov, C. Dragoiu, P.R. Dudero, J. Faulkner, K. Kovitanggoon, S. Kunori, S.W. Lee, T. Libeiro, I. Volobouev

Vanderbilt University, Nashville, USA
E. Appelt, A.G. Delannoy, S. Greene, A. Gurrola, W. Johns, C. Maguire, Y. Mao, A. Melo, M. Sharma, P. Sheldon, B. Snook, S. Tuo, J. Velkovska

University of Virginia, Charlottesville, USA
M.W. Arenton, S. Boutle, B. Cox, B. Francis, J. Goodell, R. Hirosky, A. Ledovskoy, H. Li, C. Lin, C. Neu, J. Wood

Wayne State University, Detroit, USA
S. Gollapinni, R. Harr, P.E. Karchin, C. Kottachchi Kankanamge Don, P. Lamichhane

University of Wisconsin, Madison, USA
D.A. Belknap, L. Borrello, D. Carlsmith, M. Cepeda, S. Dasu, S. Duric, E. Friis, M. Grothe, R. Hall-Wilton, M. Herndon, A. Hervé, P. Klabbers, J. Klukas, A. Lanaro, C. Lazaridis, A. Levine, R. Loveless, A. Mohapatra, I. Ojalvo, T. Perry, G.A. Pierro, G. Polese, I. Ross, T. Sarangi, A. Savin, W.H. Smith, N. Woods

†: Deceased
1: Also at Vienna University of Technology, Vienna, Austria
2: Also at CERN, European Organization for Nuclear Research, Geneva, Switzerland
3: Also at Institut Pluridisciplinaire Hubert Curien, Université de Strasbourg, Université de Haute Alsace Mulhouse, CNRS/IN2P3, Strasbourg, France
4: Also at National Institute of Chemical Physics and Biophysics, Tallinn, Estonia
5: Also at Skobeltsyn Institute of Nuclear Physics, Lomonosov Moscow State University, Moscow, Russia
6: Also at Universidade Estadual de Campinas, Campinas, Brazil
7: Also at California Institute of Technology, Pasadena, USA
8: Also at Laboratoire Leprince-Ringuet, Ecole Polytechnique, IN2P3-CNRS, Palaiseau, France
9: Also at Suez University, Suez, Egypt
10: Also at British University in Egypt, Cairo, Egypt
11: Also at Cairo University, Cairo, Egypt
12: Also at Fayoum University, El-Fayoum, Egypt
13: Also at Helwan University, Cairo, Egypt
14: Now at Ain Shams University, Cairo, Egypt
15: Also at Université de Haute Alsace, Mulhouse, France
16: Also at Joint Institute for Nuclear Research, Dubna, Russia
17: Also at Brandenburg University of Technology, Cottbus, Germany
18: Also at The University of Kansas, Lawrence, USA
19: Also at Institute of Nuclear Research ATOMKI, Debrecen, Hungary
20: Also at Eötvös Loránd University, Budapest, Hungary
21: Also at Tata Institute of Fundamental Research - HECR, Mumbai, India
22: Now at King Abdulaziz University, Jeddah, Saudi Arabia
23: Also at University of Visva-Bharati, Santiniketan, India
24: Also at University of Ruhuna, Matara, Sri Lanka
25: Also at Isfahan University of Technology, Isfahan, Iran
26: Also at Sharif University of Technology, Tehran, Iran
27: Also at Plasma Physics Research Center, Science and Research Branch, Islamic Azad University, Tehran, Iran
28: Also at Università degli Studi di Siena, Siena, Italy
29: Also at Centre National de la Recherche Scientifique (CNRS) - IN2P3, Paris, France
30: Also at Purdue University, West Lafayette, USA

31: Also at Universidad Michoacana de San Nicolas de Hidalgo, Morelia, Mexico
32: Also at National Centre for Nuclear Research, Swierk, Poland
33: Also at Institute for Nuclear Research, Moscow, Russia
34: Also at St. Petersburg State Polytechnical University, St. Petersburg, Russia
35: Also at Faculty of Physics, University of Belgrade, Belgrade, Serbia
36: Also at Facoltà Ingegneria, Università di Roma, Roma, Italy
37: Also at Scuola Normale e Sezione dell'INFN, Pisa, Italy
38: Also at University of Athens, Athens, Greece
39: Also at Paul Scherrer Institut, Villigen, Switzerland
40: Also at Institute for Theoretical and Experimental Physics, Moscow, Russia
41: Also at Albert Einstein Center for Fundamental Physics, Bern, Switzerland
42: Also at Gaziosmanpasa University, Tokat, Turkey
43: Also at Adiyaman University, Adiyaman, Turkey
44: Also at Cag University, Mersin, Turkey
45: Also at Mersin University, Mersin, Turkey
46: Also at Izmir Institute of Technology, Izmir, Turkey
47: Also at Ozyegin University, Istanbul, Turkey
48: Also at Kafkas University, Kars, Turkey
49: Also at Istanbul University, Faculty of Science, Istanbul, Turkey
50: Also at Mimar Sinan University, Istanbul, Istanbul, Turkey
51: Also at Kahramanmaras Sütcü Imam University, Kahramanmaras, Turkey
52: Also at Rutherford Appleton Laboratory, Didcot, United Kingdom
53: Also at School of Physics and Astronomy, University of Southampton, Southampton, United Kingdom
54: Also at INFN Sezione di Perugia; Università di Perugia, Perugia, Italy
55: Also at Utah Valley University, Orem, USA
56: Also at University of Belgrade, Faculty of Physics and Vinca Institute of Nuclear Sciences, Belgrade, Serbia
57: Also at Argonne National Laboratory, Argonne, USA
58: Also at Erzincan University, Erzincan, Turkey
59: Also at Yildiz Technical University, Istanbul, Turkey
60: Also at Texas A&M University at Qatar, Doha, Qatar
61: Also at Kyungpook National University, Daegu, Korea